Offshore Wind Turbine Installation Using a Double Slip Joint

Investigating the Installation Behavior of the Double Slip Joint During the Lowering Phase of a Wind Turbine Tower onto a Monopile

C.K.J. Liu

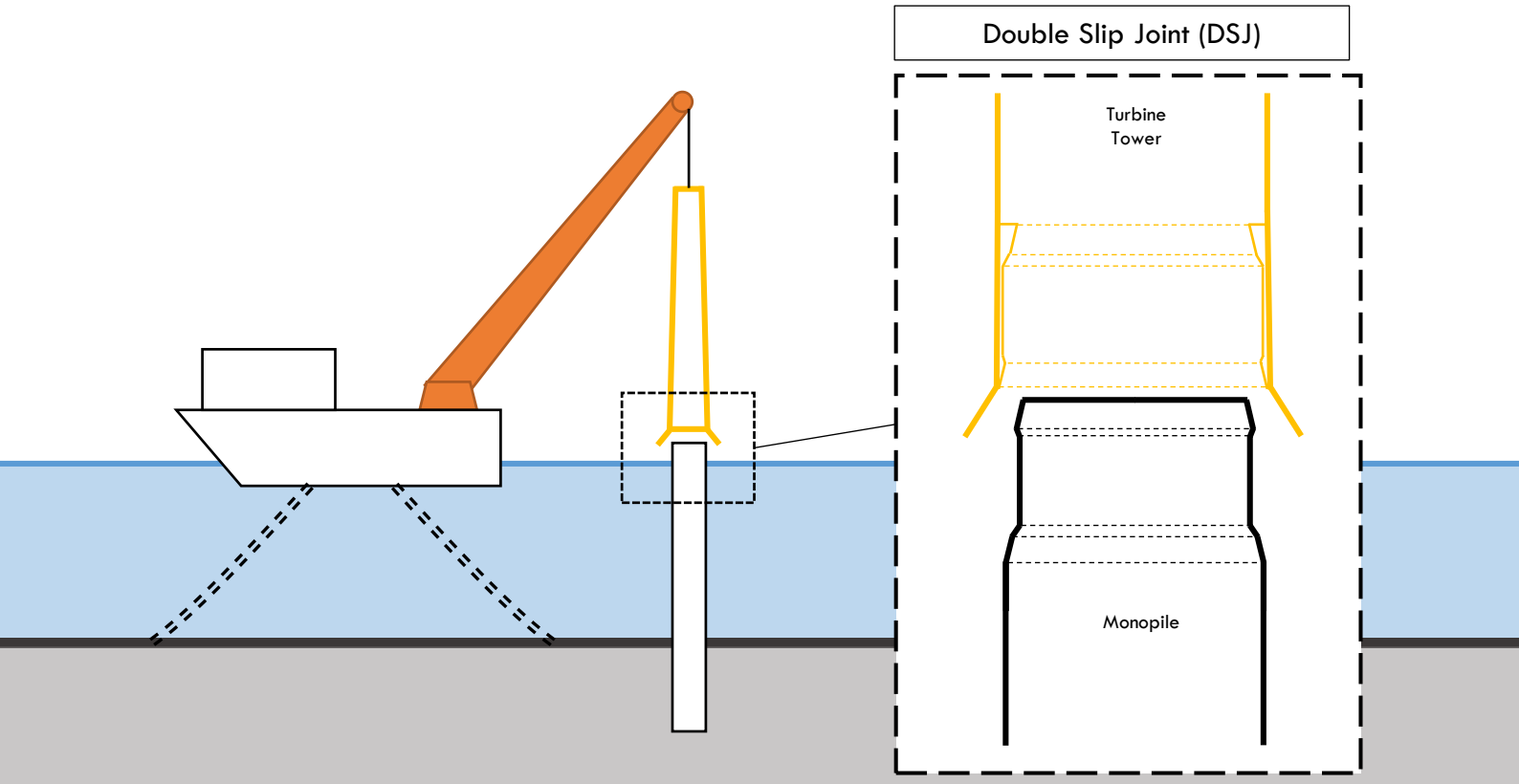

TU Delft

KCI THE ENGINEERS.

Offshore Wind Turbine Installation Using a Double Slip Joint

Investigating the Installation Behavior of the Double Slip Joint During the Lowering Phase of a WTG Tower onto a Monopile

By

Carmen Ka Jien Liu

in partial fulfilment of the requirements for the degree of

Master of Science
in Offshore & Dredging Engineering
of the Faculty of Civil Engineering, Mechanical Engineering and Marine Technology
at the Delft University of Technology,
to be defended on Thursday January 21, 2021 at 10:30 AM.

Student number: 4195051
Email: carmenkajienliu@gmail.com

Thesis committee:	Chairman	Prof. dr. A.V. Metrikine	TU Delft
	University supervisor	MSc. V. Vaniushkina	TU Delft
	Company supervisor	Ir. K.B. van Gelder	KCI The Engineers

Graduation work carried out at *KCI The Engineers*

Acknowledgement

The completion of this thesis would not have been possible without the support and guidance of my supervisor *Boudewijn van Gelder* from KCI The Engineers. Together with *Maarten van den Berg*, whose ambition and curiosity in the engineering field is truly inspiring, team Double Slip Joint was a great success. I would also like to extend my sincere gratitude to my TU supervisor *Valentina Vaniushkina* who provided me with helpful feedback on all draft versions of the report. And to the chairman of this thesis, professor *Andrei Metrikine*, thank you for your patience and the valuable feedback/suggestion you give me after each meeting. I am truly blessed to have been able to work with each one of you. And although it was a rather short period of time before the pandemic struck, I want to thank all the colleagues I met at KCI who made me feel welcome at the office and encouraged me from time to time during our coffee breaks.

Special thanks...

* To *Andrei Faragau* who gave me guidance and tips to solve the simple wire-rod problem at the very beginning of this research.
* To *Richards van der Geer* who assisted team Double Slip Joint with crucial Ansys model simulations which ultimately contributed in validating the developed Excel model.
* To *Michael James*, my thesis podcast buddy, who kept me accountable during the entire thesis, motivated me to never give up and to always find the fun in whatever we do.
* To *Pricilla Huang*, my best friend, whose support in any way meant everything to me.

Last but not least I want to thank my mom and dad. Two completely selfless human beings whose patience is as deep as the ocean and have nothing but unconditional love for their children and keep supporting each one of them in their own unique way. No words are ever enough to express my gratitude towards my beloved parents.

Carmen Ka Jien Liu
Delft, January 2021

Abstract

One of the challenges associated with offshore wind turbine installations is the mating phase. Aligning a transition piece onto its substructure under offshore conditions is a complicated and time-consuming procedure. Another issue found in a number of commissioned offshore wind turbines is related to the sustainability of the connection between the transition piece and the substructure. With wind turbines increasing in size and wind farms being built further from shore in deeper waters, the current bolted- and grouted connections are seemingly not the most suitable future proof options. This is where the Double Slip Joint steps in. A simple plug- and go connection device provided by KCI The Engineers. The Double Slip Joint's innovative solution takes away the time-consuming phases like manually fastening a number of bolts or the buffer period of waiting for grout material to fully solidify before commissioning a wind turbine. This study aims to gain more useful insights on the installation behavior of the Double Slip Joint during the mating phase under various offshore environmental conditions. The chosen system for this study consists of a hoisted wind turbine tower which is lowered onto a monopile. A numerical model for this tower-monopile system is developed in Excel where the user is able to manipulate input parameters such as mean wind velocity, tower lowering velocity, crane motions etc. After a series of validation using Ansys Finite Element models, simulations from the developed Excel model were carried out to study the Double Slip Joint's behavior during the mating phase from both a jack-up - and a floating vessel. A key finding from this study is the necessity to round off the sharp edges of the Double Slip Joints conical rings in order to avoid contact stresses that might lead to unwanted damage. The simulation results indicate that installations carried out from a jack-up vessel can be optimised to perfectly tolerate a mean wind velocity of 15 m/s, whereas that of a floating vessel can be optimised up to 13 m/s. The possibility of achieving higher mean wind velocities indicate that the weather window for offshore installations can have a greater range. The results obtained from this study confirm the potential of the Double Slip Joint for future offshore wind turbine installations.

Contents

List of Acronyms

COR Coefficient of Resitution
DAF Dynamic Amplification Factor
DP Dynamic Positioning
DSJ Double Slip Joint
DoF Degree of Freedom
EoM Equation of Motion
FE Finite Element
FEM Finite Element Method
IRENA International Renewable Energy Agency
MP Monopile
SJ Slip Joint
SWL Still Water Level
TLP Tension Leg Platform
TP Transition Piece
OWT Offshore Wind Turbine
Gacro:O & G**O & G** Gacro:O & GOil and Gas
VBA Visual Basic for Application
WTG Wind Turbine Generator

Chapter 1

Introduction

1.1 General information

In this modern era, wind energy is substantially rising in popularity among its peers. As of 2018, a major part of the total wind energy in Europe is harvested from land-based wind turbines (onshore) whereas a small part is harvested from sea-based wind turbines (offshore). This is clearly visualized in the chart from Figure 1.1 released by IRENA in a 2018 report [1]. As can be seen, the cumulative onshore generated capacity is nearly ten times more than the offshore capacity as of 2018. Looking at this chart, the growth of offshore capacity might seem insignificant in comparison to the installed onshore capacity. However, zooming in on the bigger picture, when the growth in both cases is considered separately, a better understanding of the significance and growth of offshore energy itself will be gained. The chart from Figure 1.2 offers a much clearer view on this growth.

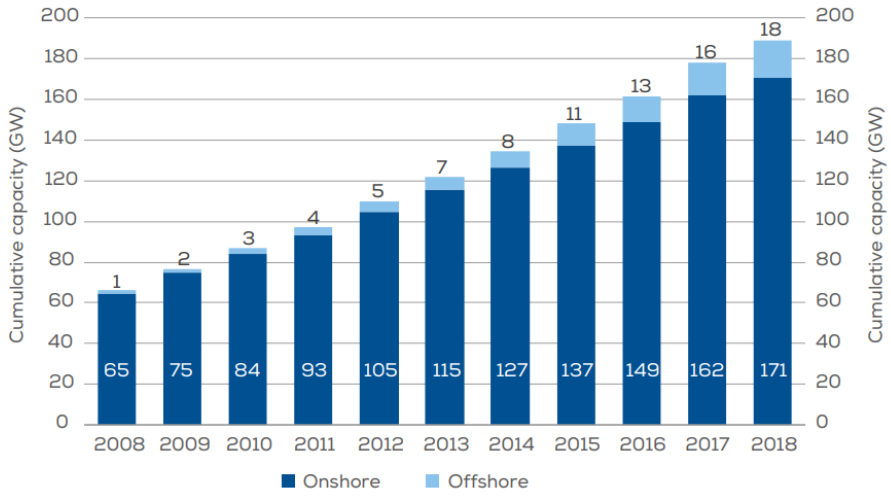

Figure 1.1: Cumulative onshore and offshore installations in Europe [1]

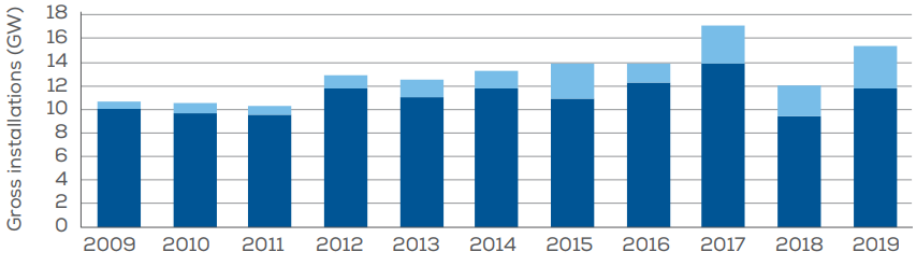

	2009	2010	2011	2012	2013	2014	2015	2016	2017	2018	2019
Offshore	0.6	0.9	0.8	1.2	1.5	1.5	3.0	1.6	3.2	2.7	3.6
Onshore	10.0	9.6	9.5	11.7	11.0	11.7	10.9	12.3	13.9	9.4	11.7
Total	**10.7**	**10.5**	**10.3**	**12.9**	**12.5**	**13.3**	**13.9**	**13.8**	**17.1**	**12.1**	**15.4**

Figure 1.2: New annual onshore and offshore wind installations in Europe [2]

In Figure 1.2, it can be seen that the portion of offshore capacity (light blue part) being installed is witnessing an increase in size whereas the portion of onshore capacity (dark blue) is more or less stagnated or even decreasing in size. In 2019, a total of 15.4 GW was installed which a significant 3.6 GW (approximately 25%) coming from offshore installations in comparison to th 11.7 GW from onshore installations. In 2018, the biggest investor in new capacity is the United Kingdom with over 90% of investments in offshore wind [1]. Besides the growth in yearly generated capacity, it seems like the offshore sector is installing further from shore and in greater water depths as time progresses (Figure 1.3). Clearly, the potential of offshore wind is not to be neglected.

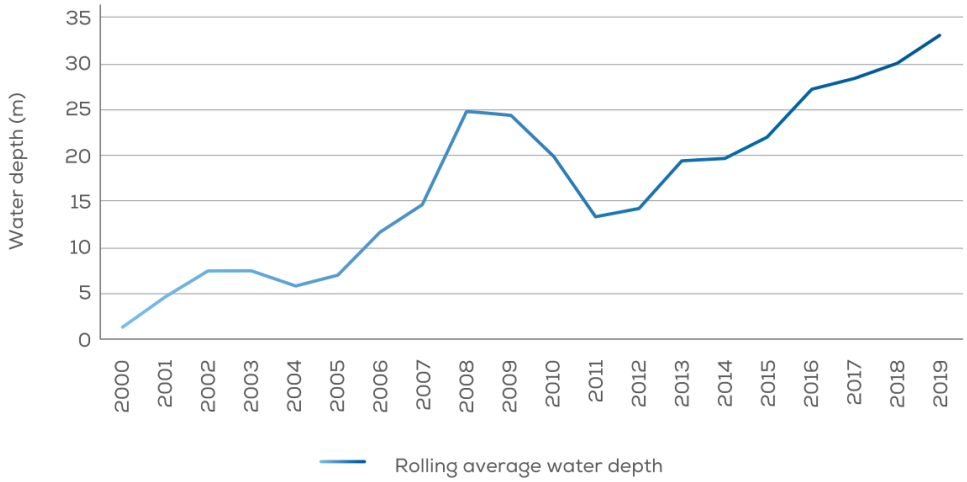

Figure 1.3: Average water depth of offshore wind farms [2]

According to a report published by IRENA in 2019 titled "Future of Wind" [2], the offshore wind industry will witness gradual growth from now until 2050. The reason why offshore wind is becoming more and more popular is because the limit is still far from sight and the potential of this option is increasing constantly as new technologies are being made such as the possibilities of manufacturing larger turbines with even higher capacities, floating structures that allow for installations at extreme water depths, wind farms increasing in size which ultimately allows for more energy being harvested etc. With all these factors in mind, future wind farms will have to shift their existence from onshore to offshore. However, this shift from onshore to offshore, comes with its own set of challenges. Two of them related to the physical structure itself are the foundation type (structure supporting the tower of wind turbine) and

the connection piece (also called a transition piece) between the foundation and the tower. These two challenges are highlighted in this report and will be elaborated more in the next sub-paragraphs.

1.2 The Support Structure

The function of this piece is to serve as the base on which the wind turbine will be installed. There are various types of support structures. Figure 1.4 shows a couple of the most common types of fixed foundations starting with the monopile on the left, then the jacket and the gravity-based. And an example of a floating foundation, a spar buoy which is fastened to the seabed by taut lines instead of hammering is also added in this illustration on the right.

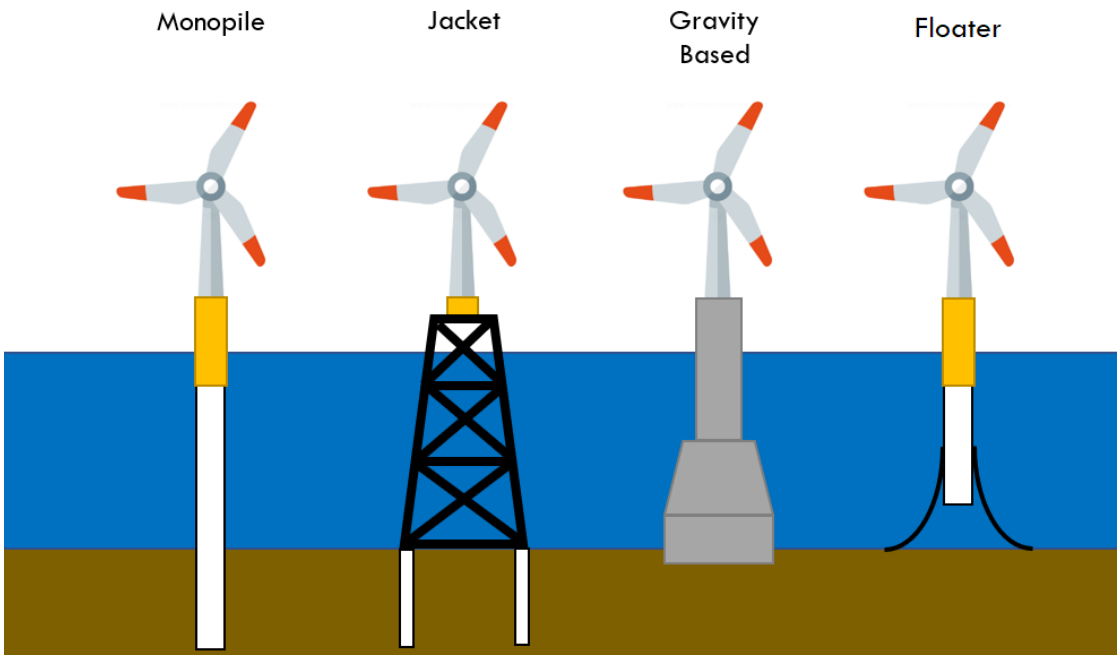

Figure 1.4: 4 types of support structures for offshore wind turbine installations

1.2.1 The Monopile Foundation

For shallow water of around 30-40m depth, the most commonly applied foundation type for wind turbine installations is the monopile. This type of support structure among its rivals is proven to be favorable due to it versatility. Its simple design, convenient shape for transportation, relatively simple manufacturing process etc. makes it the current default option for most wind farms. Figure 1.5 shows the market share of each support structure type at the end of 2017 [3]. The numbers of this chart highlights the popularity of the monopile but also approves the track-record this specific type has built up in the wind market.

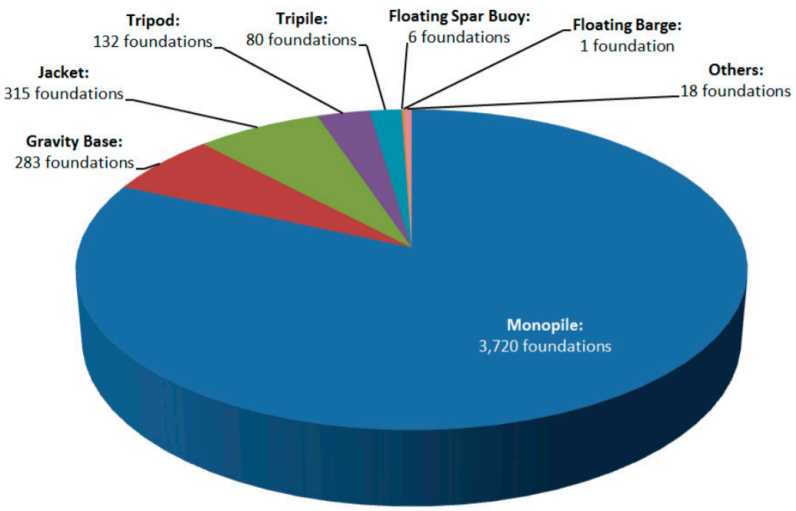

Figure 1.5: Share of substructure types for grid-connected wind turbine in Europe 2018 [3]

From the data, it should not be a surprise many of the future wind farms at much greater water depths will still be utilizing the monopile as well. However, shifting from shallow to deeper waters will require monopiles with extremely large diameters due to the harsher marine conditions. As of today, with current technologies diameters in the range of 10m are still within manufacturing capabilities. While this may be true, the challenges regarding capable transportation to the site and suitable installation vessels for lifting and hammering still remain. Even if installation is successful, monopiles with extreme diameters under harsh weather conditions might experience resonance due to the risk of the structure's natural frequencies matching with the wave frequencies. This is another potential issue that requires some more research and optimisation. Nevertheless, this popular type of support structure will still be applied for many years to come regardless of the size and weight problem [4].

1.2.2 Jacket Foundations

From the pie chart in Figure 1.5 the jacket foundation type is the second most popular after the monopile. This is not without reason. This type of support structure has built its track record from the oil and gas industry. It's welded tubular frame design makes it very transparent structure. Typically, the jacket consists of either 3- or 4 legs fastened to the seabed by driving piles through the jackets legs. This design's larger footprint compared to the monopile (Figure 1.4) makes to easier to process the overturning or bending moments. However, the high number of nodes due to the brace patterns also leads to complex and time-consuming fabrication. An example of an existing wind farm with the jacket as foundation type is the Beatrice Offshore Wind Farm.

1.2.3 Gravity Based Foundations

Compared to the jacket, gravity based foundations are less transparent. They rely on their self-weight and robustness to withstand the external loads such as overturning moments caused by the present wind and waves. The heavy base is essentially a made up of concrete material with reinforcements. However, this type of structure is usually installed in water depths of less than 10 m [5]. For greater water depths, this option seems to be less attractive due to the structure having to acquire a much greater weight to deal with harsher loads further offshore. Therefore, the gravity based foundation is not really suitable for deep water applications.

1.2.4 Floating Foundations

To expand the possibilities even more, floating structures seems to have extremely high potential for future wind farms as well. These structures are slowly integrating into the wind sector as technology advances and more insights are gained from several pilot tests which are currently under development with the aim of commercialising it in the near future. A crucial advantage on why the floating foundation can be a game changer for the offshore wind market is ability to eliminate the water depth constraint. Without this constraint, deeper waters will become more accessible for future installations. Especially for countries with limited shallow water areas, the floating foundation is an extremely attractive option. Figure 1.6 shows the main categories of floating structures are spar buoy (also illustrated in Figure 1.4), semi-submersible and Tension Leg Platform (TLP). Table 1.1 gives an overview of these main categories and their difference in stabilisation mechanism.

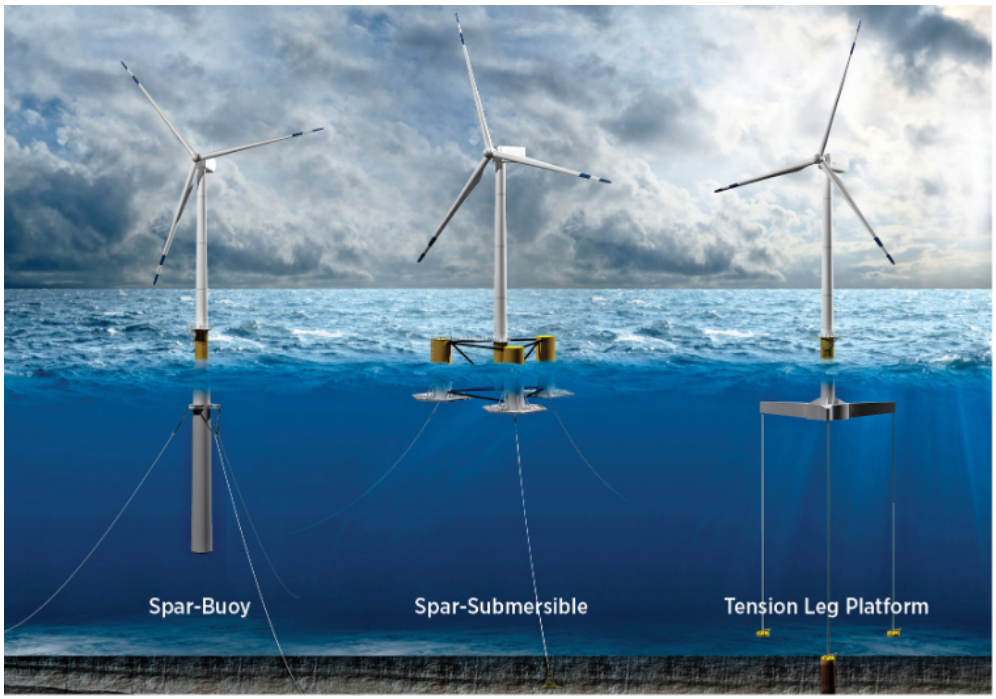

Figure 1.6: Offshore wind floating foundation concepts [6]

	Floater type	**Stabilisation Mechanism**	**Water depth**
1	Spar buoy	Ballast	$>$ 100 metres
2	Semi-submersible	Buoyancy	up to 40 metres
3	TLP	Mooring	up to 50 - 60 metres

Table 1.1: Main types of OWT floating foundations [6][7][8]

The challenge of deploying an offshore floater is keeping it stable during its whole life expectancy while dealing with extreme harsh environmental conditions. Another drawback of a floating foundation currently is the relative high cost compared to fixed foundations. According to the International Renewable Energy Agency (IRENA), the motivation to develop floating foundations is that it makes deeper water areas accessible which then allows for large scale wind farm deployments and (in the near future) potentially easier and simpler installation of an OWT due to the unnecessary harsh invasion of the seabed for pile installation [6].

1.3 The Transition Piece

This type of connection was commonly used in the Oil and Gas (O&G) industry. Due to the positive reputation from the O&G industry, it quickly became a crucial part for the installation of offshore wind turbines (OWT) as well. Aside from being a vital connection between the turbine tower and the monopile (MP) it is also there to compensate for the possibility of a not fully vertically hammered MP [9]. The TP is placed/sleeved on the MP, with a sufficiently accurate vertical orientation and then fully fastened by either grout or bolts. The TP then takes on the role to assure that the turbine tower which is installed on top is accurately vertical. Figure 1.7 shows the typical arrangement of a TP as a connection between the tower and the MP.

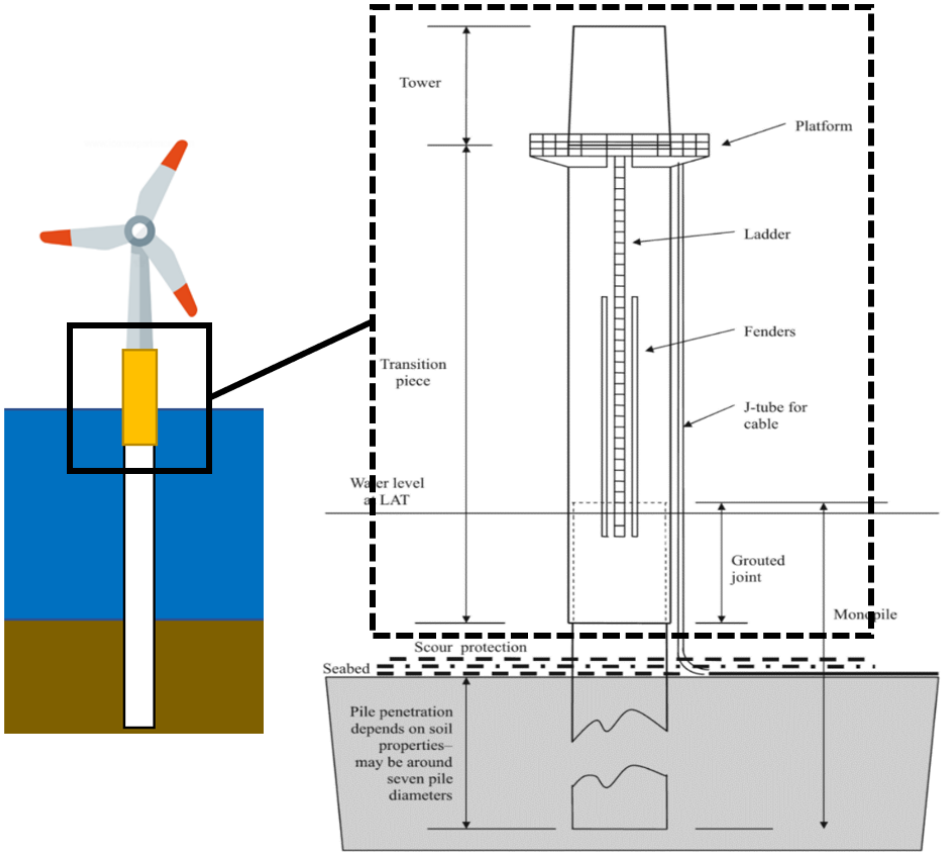

Figure 1.7: Typical arrangement of monopile and transition piece [10]

As mentioned, the TP can be either fully fastened by grouting or bolting. Both of these fastening methods are also adopted from the O&G industry. The only difference between the TP application on an O&G platform and an OWT is the loading regime on the substructure. The latter experiences loads in a much more dynamical sense (mainly due to a rotating rotor) whereas the former is a more robust and static jacket platform. The dominant load a MP experiences are bending moments caused by a combination of wave and wind [11]. More details on grout- and bolted connections will be given in the next sub-paragraph.

1.3.1 Grouted - & Bolted Connections

During an OWT installation, the TP is placed over the hammered MP. The way this TP is fastened to its substructure is done by various types of connections. In case of grouted connection, it is achieved by fill-

ing in the gap between the overlapping TP and MP diameter with High-Strength cementitious Grout and waiting for this filling to cure and fully fasten both cones. Therefore, the function of this grout is to serve as a binding material between the two cylindrical cones to avoid further motions due to gaps (a tube-in-tube connection) [12]. This method is directly adapted from the O&G industry where it was found to be working properly. However, the lack of accounting for bending moments in dynamical OWT cause by combinations of wave, wind and turbine motions in the design consideration resulted in numerous grouted connection failures (settlement) that has been discovered around 2010 [13][14]. An example of where grout failure is discovered is the Princess Amalia Wind Farm (Figure 1.8). The solution to this problem was the design of pilot repair plan which was applied on all the foundations of the wind farm. This ultimately resulted the need to invest an additional €47 million for reparation purposes [13]. Since then, grouted connections have been improved with shear keys to or even a conical shape to increase resistance against sliding to prevent unnecessary settlement.

After these failure cases, a substitute solution for these grouted connection has been found in bolted flanges. Currently, bolted flanges are a very common solution seen in wind turbine structures and gradually becoming the default option in connecting the TP to the MP. Compared to grout, bolted flanges are more superior because problems seen in the former such as slippage and cracking are altogether avoided due to the fact that the loads are now transferred directly from steel cone to steel cone without the cylinders overlapping each other. Even though the bolted flanges seems to fix all the issues seen in grouted connections, it also comes with some flaws that should be carefully taken into consideration. Some crucial ones being [13]:

- High sensitivity to corrosion due to exposure and thus requires additional protection to achieve the wanted lifetime
- The need for applying the right tension to the bolt and closely monitoring this to prevent this tension from falling
- Time consuming (which directly affect the costs) due to the large number of bolts, especially with increasing structure diameter.
- Challenges associated with upscaling these bolted connections with increasing turbine sizes.
- High precision is required during the lowering process to match up the bolt holes between the TP and the MP.
- The axial impact during touch down should be carefully controlled to avoid significant damage.
- After matching up the bolt holes, the connection is not stable yet. The TP should be kept stable for a period of time sufficient for the engineers to fasten all the bolts.

In Figure 1.8, a grouted- and bolted connection is illustrated.

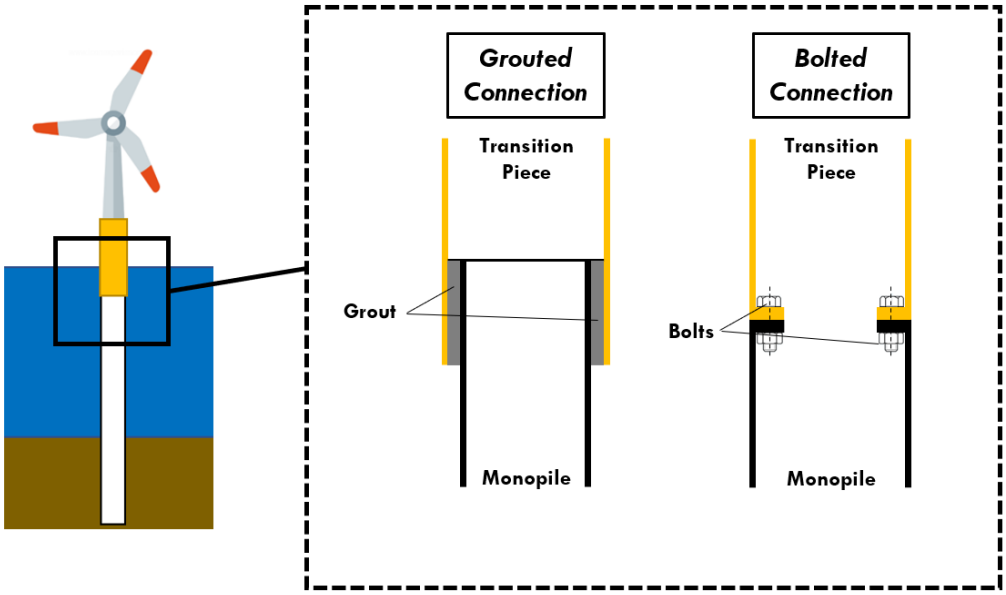

Figure 1.8: Grouted- & Bolted Connection

1.3.2 Conclusion

The aforementioned grout and bolted flange options to fasten a TP to the MP are therefore not the most efficient and cost-effective options for future installations involving extremely large cylindrical diameters and extreme marine conditions where the installation time should be kept as short as possible. To avoid similar failure cases and to find more efficient methods, innovations had to be developed.

1.4 The Double Slip Joint

1.4.1 Introduction

KCI The Engineers came up with an innovative solution to bridge the gap in a more efficient way with the wind sector's future in mind - the Double Slip Joint (further abbreviated as DSJ).

The DSJ is a connection device developed for quick and safe installation of a TP and/or and Offshore wind turbine (OWT) on its substructure. This design is inspired by the Slip Joint (SJ) connection which in the past is typically seen in installations on smaller onshore turbines up to 700 kW. The most simple analogy to describe the SJ's design is stacking one cup over another in their flipped orientation. The DSJ on the other hand is slightly modified by adding two sets of rings attached to the cones. Both the SJ and DSJ illustrated in Figure 1.9.

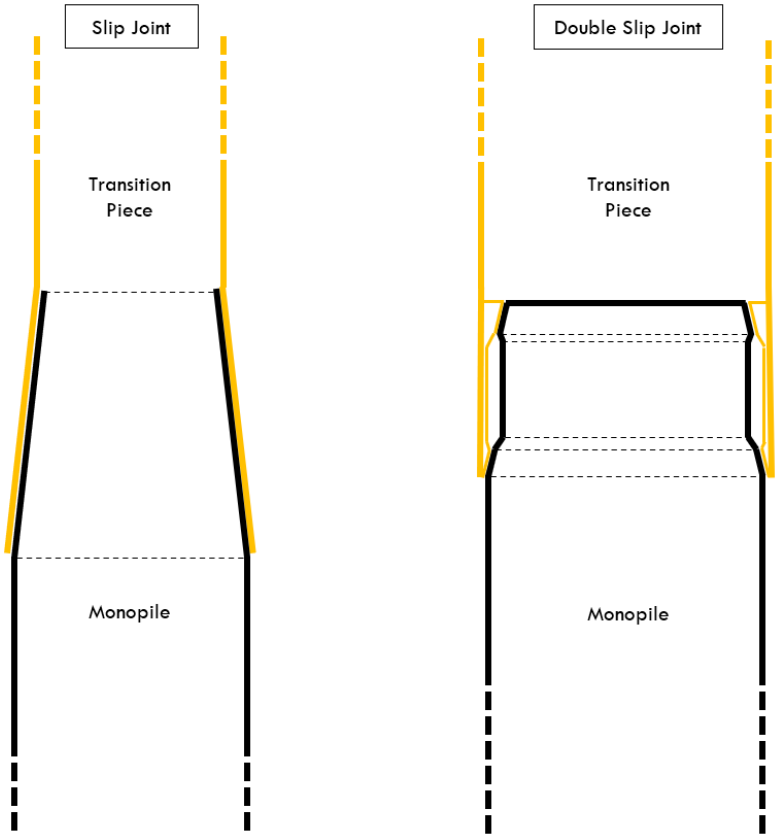

Figure 1.9: Cross-section of the Slip Joint & Double Slip Joint

From Figure 1.9 it is obvious that the SJ's contact area after successful installation consists of a large but undefined surface (tapered cone) whereas the DSJ's contact area is only limited to the two sets of conical rings (tapered rings), hence the name Double Slip Joint. Focusing the contact area solely on the rings enables well defined contact.

1.4.2 Settling behavior of the Slip Joint

In 2014, a study conducted regarding the settlement of the SJ showed that the desired settlement level is not reached just under the self weight of the upper cone for the tested conditions. Even with a velocity of 1.4 m/s at the time of contact (by dropping the upper cone from a small height) the settlement was insufficient as shown in Figure 1.10. Increasing the contact velocity is not desirable as it might lead to unwanted damage of the structure due to the impact load. [15].

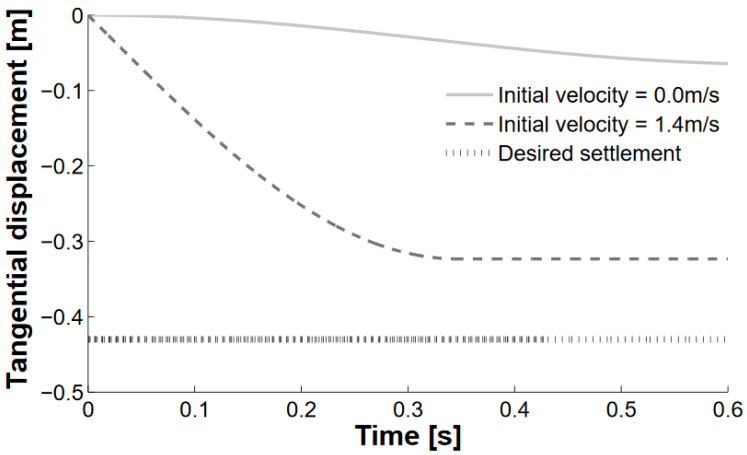

Figure 1.10: Settlement level under self weight with and without initial velocity [15]

In order to find a solution to improve the settling behavior, a study regarding the potential of applying harmonic excitation during installation and the effect it has on the SJ's settling behavior was carried out. This study showed that in order to achieve a proper fit between the cones of the SJ, applying a harmonic load with specific vibrational frequencies is required (Figure 1.11). This is an indication that the settling part of the installation process can be controlled to achieve proper fit between the cones [16].

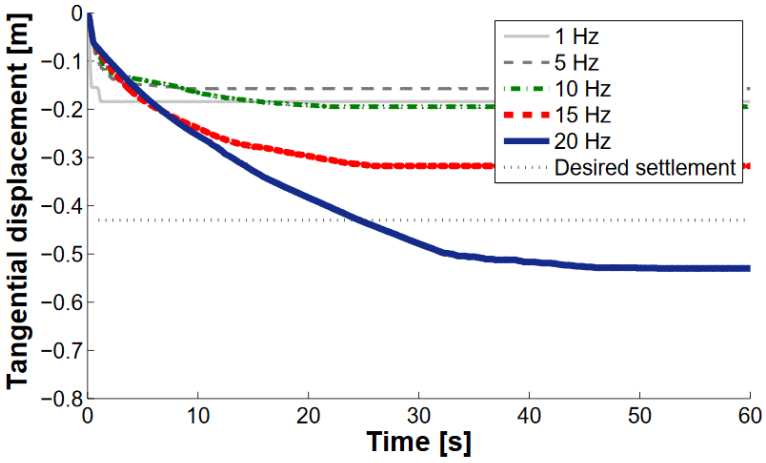

Figure 1.11: Settlement level under harmonic loading for various frequencies [15]

1.4.3 The advantages of the Double Slip Joint

The DSJ was developed taking all previous failure events seen in grouted - and bolted connections into consideration. This design does not involve any grout material or bolts for fastening purposes. It is designed with simplicity and efficiency in mind and is therefore based on a plug & go principle. The transition piece (or tower) is lowered on the monopile and the connection is self-interlocking due to its own weight (TP or tower). In comparison to grout and bolt, this solution is less time-consuming and more cost-efficient. Another noteworthy advantage of a DSJ connection is less safety issues compared to

bolted connections where engineers need to be physically working inside the turbine to fasten the bolts. Comparing the DSJ with the SJ, some noteworthy advantages are summarized in the list below.

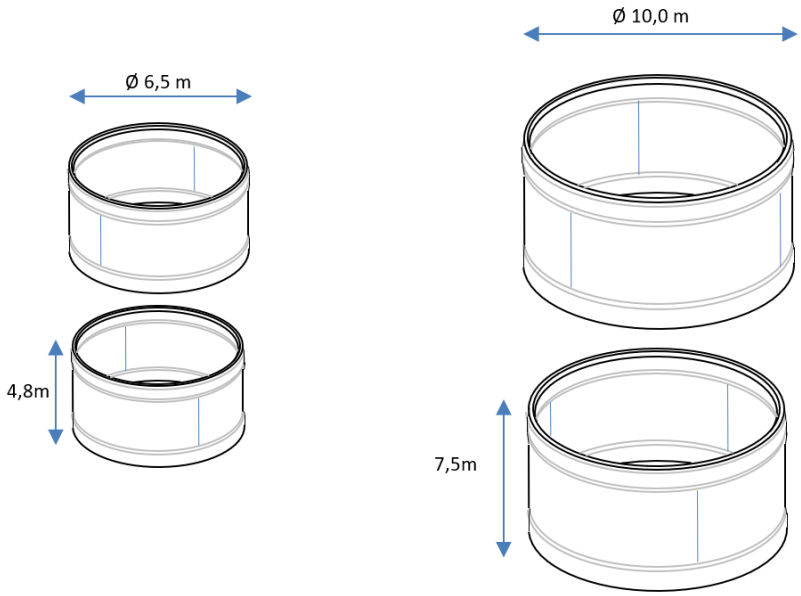

Figure 1.12: The DSJ pieces

The advantages of the DSJ summarized are:

- Compact device
  Mass-wise, the SJ's cone design is a rather heavy part of the complete structure due to its height and surface area. On the other hand, the DSJ is designed to be compact, lightweight and economical. It is a device that can be ordered separately and then mounted/welded to the relevant pieces that needs a connection.
- Simple fabrication
  The design of the DSJ is fairly simple with no complicated shape. Therefore, allowing an automated assembly process during fabrication, and supply as a pre-fab element for the foundation.
- Closed connection
  The contact area after applying the SJ is not well-defined. The potential gaps between the overlapping cones might lead to corrosion issues in the future if sea water is seeping through the connection's gaps. This issue can be prevented by using filling material to close the gaps. Due to the two sets of conical rings (machined forgings) on the DSJ, the connection is basically sealed after installation disabling any flow or seawater going through preventing corrosion fatigue.
- Conical rings with well defined contact
  As mentioned before, the contact area of the DSJ is solely located at the two sets of rings. Focusing the contact area on the rings specifically enables a design such that slip movements will stop after a short period of self-settling.
- Under water application possible
  Owing to the fact that this design is based on a plug & go principle without the need of any staff at the connection part during installation, this is theoretically applicable under water.

1.4.4 Milestones

The DSJ development started back in 2014 with a Finite Element Model (FEM) in Ansys and studying its mechanical behavior [17]. In 2015, a follow up project was done studying the settling behavior of the DSJ by means of an experimental set-up. This experimental research confirmed the self-locking behavior (for all the loads tested in the experiments including irregular environmental loading) of the DSJ and was used to make several essential adjustments and refinements of the numerical FEM model. It was also concluded the DSJ settles through slip motions and comes to a stand still when it is fully fastened (the slip then reduces to zero) [18]. In 2016, the possibilities to further optimize the DSJ for fabrication by testing various design geometry parameters is investigated [19].

1.5 The Offshore Challenge

Lifting any object (TP, turbine blade, tower) under offshore conditions with the aim to install it at a very specific location is an extremely challenging task. This is especially the case when a floating vessel is utilized under certain wind and wave conditions. The motions of the crane tip will directly affect the entire lifting system's responses [20]. The mating phase of offshore processes has always been a challenge. This is also proven to be the case according to a research paper released in 2019. This paper mainly addresses the consequences of the impact loads experienced during the mating process between a wind turbine blade and the hub. This research was conducted based on a realistic scenario of a one blade model using tugger lines being installed on to a pre-installed monopile structure [21]. However, the limits of a wind turbine blade installation can be more demanding due to the relatively small and more fragile guide pin and blade root connections (Figure 1.13) compared to the installation of a massive TP onto its substructure.

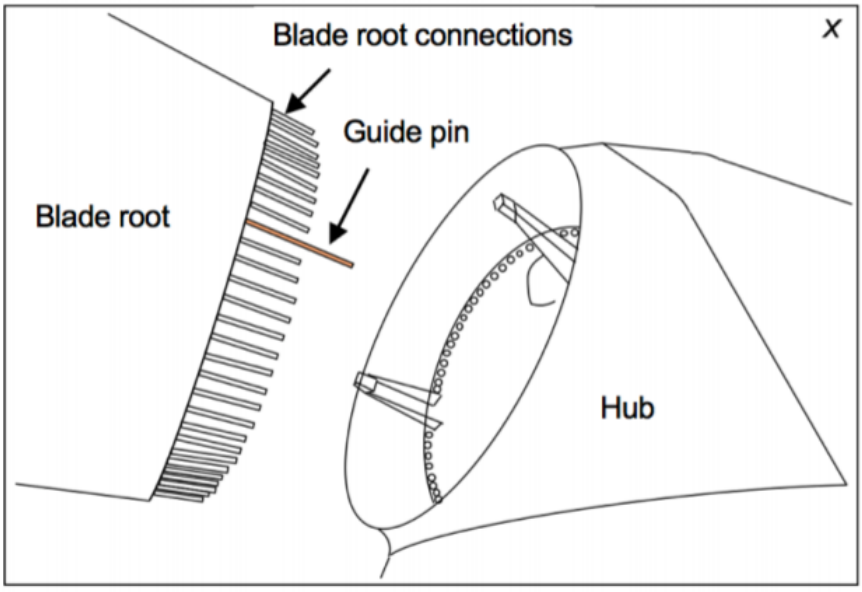

Figure 1.13: Magnified view of the blade root and the guide pin [22]

Although, TP installation may seem less risky compared to the delicate blade root connections, it is not necessarily the case. A paper released in 2014 by Li et al. studying the eccentric - and inclined vertical impact between a TP and the monopile during installation from a floating vessel shows that significant plastic deformation can occur axially as illustrated in Figure 1.14 [9]. This might lead to unacceptable damage of the structure, causing unsuccessful installation and therefore delaying the project. In order to avoid or limit the potential risks of damaging any part of the structure, the environmental (external)

loads affecting the motions of the system need to be considered carefully alongside the object that is to be installed. For new concepts like the DSJ, more insights are required regarding the dynamic behavior of this device during the mating phase in the marine environment.

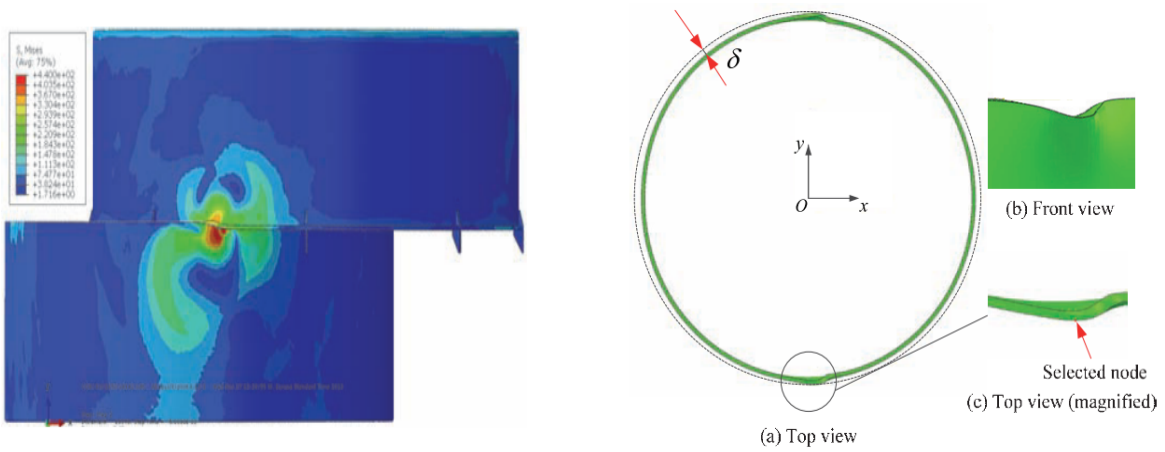

(a) Front view **(b)** MP top view

Figure 1.14: Axial impact between a TP and MP [9]

1.6 Thesis Framework

The framework of this research is discussed in this chapter. Starting off with the problem formulation where the problem definition and the objective will be addressed, and the scope and research questions of this thesis are defined. In the second paragraph, an overview of the report structure is given. This chapter is finalized with a last paragraph explaining the approach/method applied during this project.

1.6.1 Problem Definition

The main problem identified after a general overview of the current status is that the impact loads and potential risk of damage during the *mating phase* from an installation vessel between the turbine tower and its substructure by means of a DSJ, is still unknown. Especially when these installations happen under the marine environment concerning wave- and wind loads of varying amplitudes. The crane vessel along with the lifted turbine tower will have certain wave-induced motions which is not negligible during the entire installation process. Additionally, the substructure is also prone to wave loads and will exhibit motions regardless of foundation type. In the case of a monopile foundation, the (wave-induced) motions of the top of the pile will substantially be less due to its bottom-founded (fixed) characteristic compared to a floating substructure moored or fastened to the seabed with much more motion in the various degrees of freedom.

The mating phase of the DSJ is mainly covering the interaction (dynamics) between the lifted turbine tower and its associated substructure. The response of the two upon first contact until full contact with certain initial conditions such as a swinging turbine due to weather conditions and a (slightly) moving substructure either due to the wave loads or its characteristics is yet to be investigated. This impact phenomena is surely a complex dynamic problem and needs to be addressed as it is of great importance and value for the future offshore applications of the DSJ. Therefore, more in-depth research covering the impact phenomena during the mating phase is required in order to make sure future installations will be safe and successful.

1.6.2 Objective

The objective is to determine the behavior (dynamics) of the Double Slip Joint during installation (from first contact between the DSJ rings until the final position as shown in Figure 1.16). Study the effect of various initial conditions (lowering speed, wind load, crane tip motions etc.) on this behavior and find the allowable limits that determine a successful installation.

1.6.3 Research questions

After formulating the objective, the research question of this thesis is can be carefully constructed as:

"What is the installation behavior (dynamics) of the Double Slip Joint during the mating phase, in particular from first contact between the DSJ rings until the final position?"

The following sub-questions are formulated for partial studies to help answer the research question:

1. What type of model is suitable to represent the system sufficiently?
2. How can the impact phenomena be modelled? (impact detection & material stiffness estimation)
3. What should this model deliver as relevant outputs?
4. How can this model be validated?
5. How can the validated model's output be utilised to answer the main research question?

1.6.4 Boundaries & scope

As mentioned previously in the problem statement and objective, the focus of this thesis is going to be from first contact between the DSJ rings until the final position. However, acceptable assumptions are required for the processes prior to the mating phase (e.g. crane tip motions, wind loads on the turbine tower etc.) to ensure a realistic mating phase. Therefore, the boundaries and scope of this research are established as follows:

1. *The Model*
   The model which will be built during this research will be of 2-dimensional nature. This is a good and simple starting point to study the behavior of the mating phase. Another advantage of a 2D simulation is easier visualisation compared to 3D especially when a contact problem is being considered. A basic schematic model of the system is depicted in Figure 1.15.

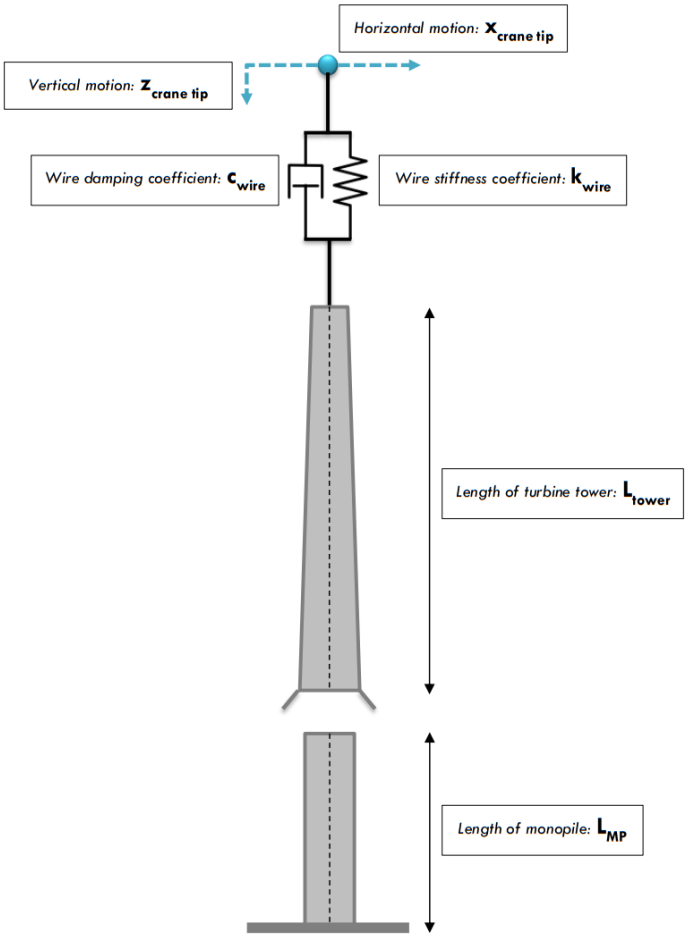

Figure 1.15: Schematic model of the Tower-MP system

2. *The vessel and crane tip*
   As this research focuses mainly on the mating phase of a wind turbine with a DSJ, and not the coupling between the vessel motion and the crane motion, the vessel's motion will be translated to crane tip motions for simplicity. Therefore, the installation vessel's motion under offshore environmental conditions will be taken into consideration by having adjustable crane tip amplitude and frequencies in the model in both the vertical and horizontal direction. The crane tip motions will be assumed based on initial literature review and advice from industry professionals and on a later stage adjusted and refined based on the research of Maarten van den Berg happening simultaneously alongside this research.

3. *Lifting Wire*
   The lifting wire that will be used in the model will have a variable length to account for the lowering process and the following properties listed in Table 1.2.

Stiffness top	k_{wire}	3E+07	N/m
Damping	c_{wire}	187333	Ns/m

Table 1.2: Lifting wire specifications

Note, that the wire properties used for this research are constant values and represents a specific wire material. Which affect the natural frequencies of the entire lifting system. Therefore, for future optimisations of the lifting process, it is recommended to choose a more optimal

4. *The turbine*
   Since the DSJ is a two part device, the first part of the DSJ is mounted/welded on the bottom of the turbine. And for this research, the turbine will be of the following geometry and specifications listed in table 1.3.

Tower length	L_{tower}	129.1	m
Diameter top	D_{top}	5.5	m
Diameter bottom	D_{bottom}	8	m
Wall thickness top	t_{top}	35	mm
Wall thickness bottom	t_{bottom}	70	mm

Table 1.3: Turbine tower specifications

5. *The Support Structure*
   The second part of the DSJ is mounted/welded on the top of the support structure. The motions of this will be addressed and included in the analysis by means of a simple generic model with adjustable amplitude and frequencies to mimic the wave loads affecting the support structure. The scope of this research will only cover the monopile foundation as it is the simplest and most popular option. The monopile specifications are listed in Table 1.4.

MP length	L_{MP}	60	m
MP Diameter top	D_{MP}	7.85	m
Wall thickness top	t_{top}	80	mm
Wall thickness bottom	t_{bottom}	110	mm

Table 1.4: Monopile foundation specifications

6. *The mating phase*
   The phase describes the activity of connecting the turbine and its substructure by means of a DSJ and covers the interaction between the turbine tower and its substructure. For this research, the mating phase is specifically starting from the moment the tower's lower DSJ rings touches the MP's upper DSJ ring until fully installed (DSJ fully matched up) as illustrated in Figure 1.16.

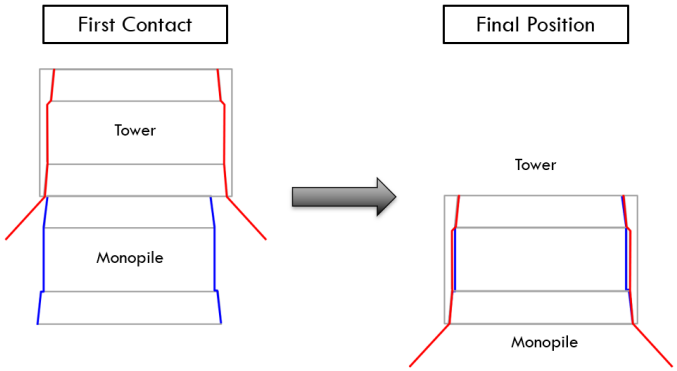

Figure 1.16: Mating phase definition

7. *The DSJ geometry & dimensions*
The geometry and specific dimensions of the DSJ that will be used to conduct this research is listed in Figure 1.17 and Table 1.5. These values are scaled up based on a DSJ concept version with diameter of 6.5m.

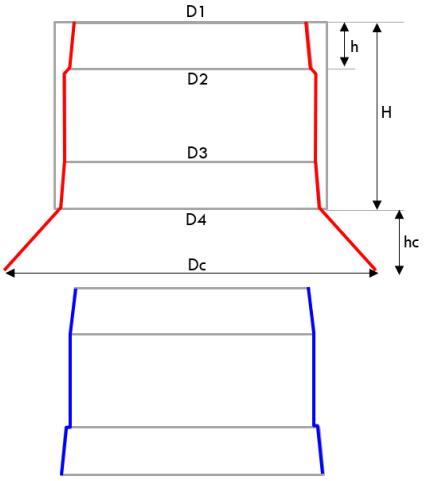

Figure 1.17: DSJ Geometry

Diameter top ring	D_1	7.85	m
Diameter top ring	D_2	7.91	m
Diameter bottom ring	D_3	7.92	m
Diameter bottom ring	D_4	8.00	m
Diameter catcher	D_c	10.00	m
Catcher height	h_c	1.00	m
Ring height	h	1.00	m
DSJ height	H	6.00	m

Table 1.5: DSJ Dimensions

1.6.5 Research Flowchart

This research is divided into several parts. The flowchart depicted below gives the general approach to achieve the objective.

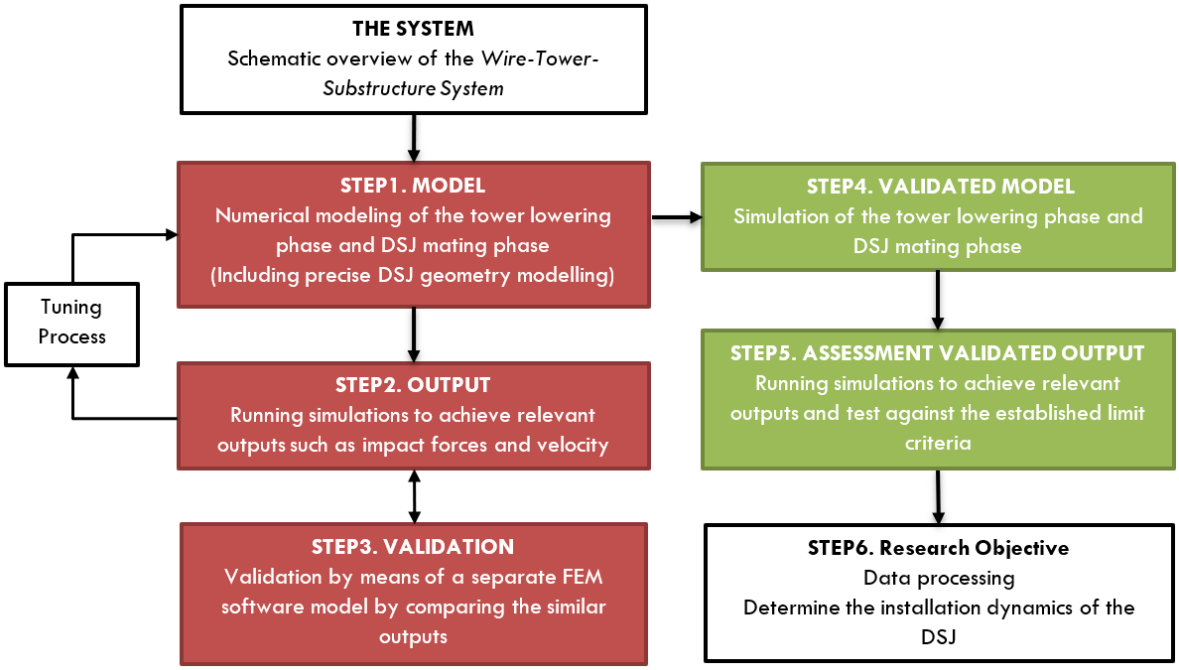

Figure 1.18: Flowchart

Step 1. Model
As the main objective is to investigate the mating phase by evaluating parameters such as maximum velocity at the moment of impact (further referred to as "*impact velocity*"), impact force, allowable stresses etc, the ultimately built model should be user-friendly when it comes to adjusting the input parameters. The program should be simple and not a black box. The components built in this program/system should be available for inspection. The most obvious option at the time of the research (both due to the simplicity and logistical reasons) is Microsoft Excel. This software is capable of creating animations using the macro or VBA feature by means of loops or code lines. For validation of certain parameters like stiffness and damping concerning material behavior during impact, separate specific models can be built in Ansys Workbench based on the Finite Element Method (FEM) principle. In this step of the flowchart, the base case of the Tower-MP system as depicted in Figure 1.15 is thus modeled in Excel. This model includes the adjustable parameters mentioned in the Boundaries & Scope part of this report (section 1.6.4). The general behavior of the swinging tower is validated in this step solving it as a wire-rod pendulum system. For the collision part, a first assumption will be made of the stiffness and damping coefficients based on literature values.

Step 2. Output
This step consists of the results obtained from the base model. Results will be in the form of time simulations of the mating phase in the form of impact forces.

Step 3. Validation
The goal of this step is to validate the motion behavior of the system caused by impact and the magnitude of the impact forces that occurs. This is done by comparing the created Excel model with Ansys models covering the same base case (Tower-MP system). An attempt will be made to adjust the Excel model in order to match up with the more realistic Ansys model by tuning parameters such as the stiffness - and damping coefficients that covers the collision behavior (most left rectangle in the Flowchart depicted in Figure 1.18).

Step 4. Validated Model
After a validated model (with the best estimate/tuned values to mimic the collision behavior), more simulations can be run while varying the initial condition parameters such as vertical - and horizontal crane tip motions, lowering speed, wind speed etc.

Step 5. Assessment Validated Output
This step consists an assessment of the results generated from the simulations in Step 4 by means of the established criteria.

Step 6. Research Objective
With the obtained data generated from the simulations, more insights will be gained on the mating phase while using a DSJ as a connection device.

1.7 Thesis Structure

The first chapter contains some background information and introduction of the Offshore Industry and its developments. And narrowing it down to the objective of this thesis, the chapter concludes with the research approach and methodology. Chapter 2 covers the literature study part in which theories relevant to this thesis are reviewed. Chapter 3 contains an elaborate explanation of how the model is built and what it is capable of with its features. The validation of this model is covered in Chapter 4 with some Ansys FEM models. After a validated model, the output results can be assessed with the criteria elaborated in Chapter 5. Chapter 6 is the result of Chapter 4 and 5, where a range of simulations with the validated model for both jack-up - and floating vessel are investigated and tested against the established criteria. Last but not least, conclusion and recommendation are given in Chapter 7 and 8 regarding the findings of this thesis. This thesis structure is summarized in the flowchart below:

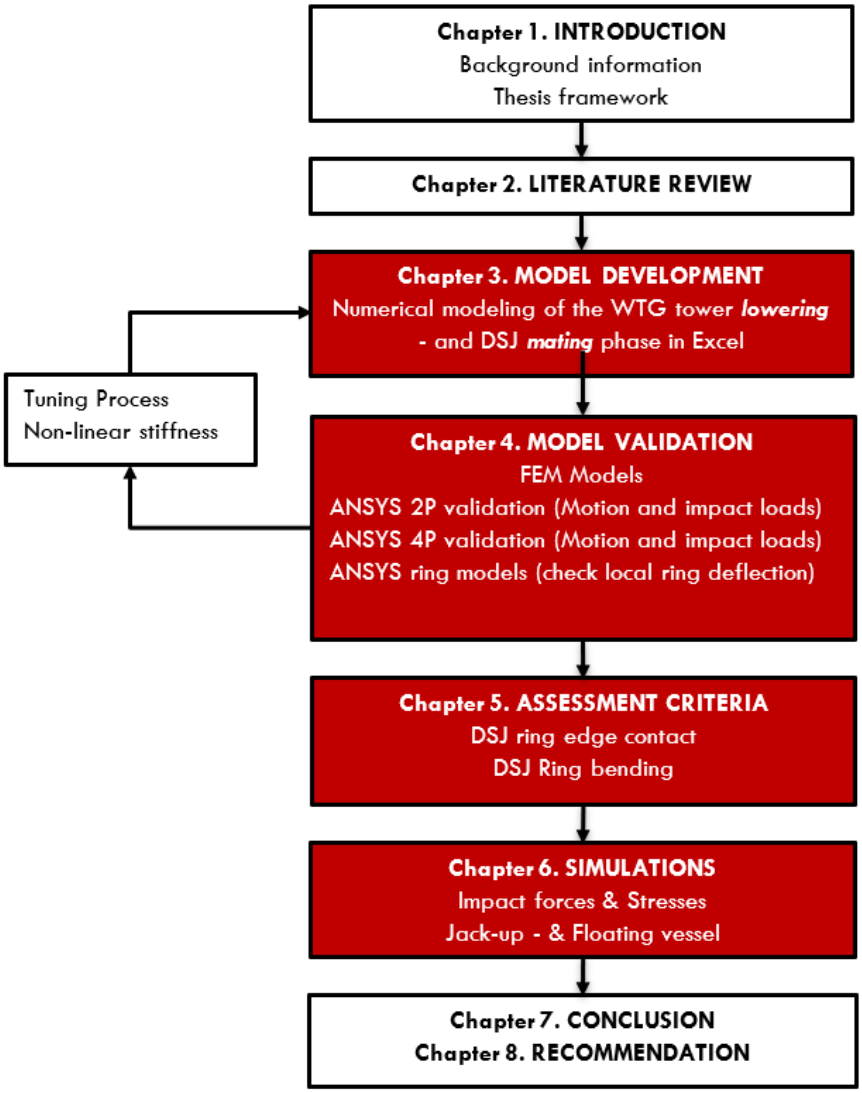

Figure 1.19: Thesis Structure

Chapter 2

Literature Review

This chapter provides a summary overview of the existing studies or theories reviewed prior to the model development phase.

2.1 Manual Numerical Simulation

Animated time simulations in Excel can be done by summing up all the calculated time frames. This specific method of solving a numerical problem with Excel is rather unique and has not been done widely. However, research shows that many problems ranging from simple mass-spring-damper systems to complex 3D flight simulators can be solved/animated with Excel [23]. Various numerical methods can be used to calculate the time frames by solving the differential equations. For any numerical method, discretization is required. In any case, the total simulation or video time will be discretized into time steps. The general notation for length between each frame is δt. The smaller this δt, the more smooth and continuous the video will turn out and therefore resulting in a more realistic simulation. However, the downside of choosing a very small δt is longer computation times due to the higher number of frames and therefore more time-consuming. Hence, choosing the appropriate numerical method and time step is of high importance.
In order to generate this animated time simulation in Excel, two things need to be considered carefully:

1. Method to determine the equations of motion of the system (Section 2.1.1)
2. Method to solve equations of motions for every time step (Section 2.1.2)

2.1.1 Motion of the system

Two options are assessed for this topic: *the Lagrangian* - and *Moment Balance Method.* Both these methods are applied and compared for a simple wire-rod pendulum system as seen in Figure 2.1 (detailed description in section 2.2).

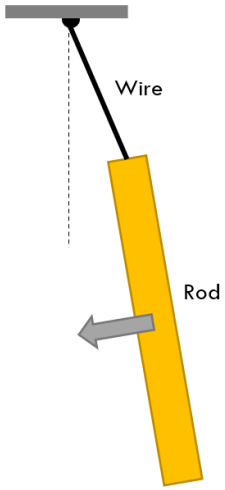

Figure 2.1: Simple wire-rod pendulum system

The Lagrangian Method
This first method solves the system's equations of motion by deriving it from the potential and kinetic energies. First, the relevant coordinates of the system with respect to an assumed reference point are defined. Second, the kinetic and potential energy will be assembled based on the predefined coordinates. The Lagrange equation can then be expressed in terms of the kinetic - and potential energy as presented in Equation 2.1. The equation of motion (EoM) for each degree of freedom (DOF) of the system can then be solved by taking the associated derivative of the Lagrange equation as presented in Equation 2.2.

$$\mathbf{L} = \mathbf{K} - \mathbf{P} \tag{2.1}$$

- **K** is the kinetic energy of the system
- **P** is the potential energy of the system

$$\frac{d}{dt}\frac{\delta \mathbf{L}}{\delta \dot{q}} - \frac{\delta \mathbf{L}}{\delta q} = Q \tag{2.2}$$

- q(t) represents the degree of freedom of the system
- Q(t) is the force acting on the system

The Moment Balance Method
The wire-rod pendulum system will be expressed in both translational and rotational (angular) motions. The first can be derived from Newton's second law which states the force equals the mass times the translational acceleration. The second one is derived by taking the sum of the moments divided by the object's (rod) moment of inertia. The expressions for both accelerations are therefore (Equation 2.3 and 2.4):

$$\ddot{x} = \frac{\mathbf{F}}{m} \tag{2.3}$$

$$\ddot{\theta} = \frac{\mathbf{M}}{\mathbf{I}} \tag{2.4}$$

- $\ddot{x}$ is the translational acceleration
- $\ddot{\theta}$ is the rotational acceleration
- **F** is the total forces acting on the system
- **M** is the total moment acting on the system
- **m** is the mass of the moving object (rod)
- **I** is the moment of inertia of the object (rod)

Both these expression will be used to determine the location of the rod's center of gravity and angle at a certain given time by integrating the accelerations twice.

2.1.2 Time Integration Method

The model will be solved using the Euler Integration Method. For a time discretized system, each time frame t_{n+1} can be solved given t_n with n being the time step between each frame. This first order numerical method is the simplest among its peers to solve ordinary differential equations given the initial value. The global error of this solver is of first order and the local error is proportional to the step size squared. The generic equation as seen in most literature is written as follows (Equation 2.5):

$$y_{n+1} = y_n + hf(t_n, y_n) \tag{2.5}$$

- y_{n+1} - time frame to be solved
- y_n - known time frame
- h - step size
- $f(t_n, y_n)$ - differential equation of y_n

2.2 The Wire-Rod System

A simple wire-rod system with be covered in this section in order to get more insight on the general motion behavior of a complex crane lifted tower system. A simple schematised version of the two degree of freedom system is illustrated in Figure 2.2.

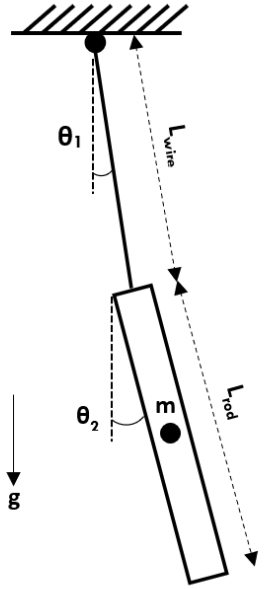

Figure 2.2: Wire-rod System

This equation of motion for this wire-rod pendulum system is solved using both the Lagrange - and Moment Balance Method.

2.2.1 The Lagrangian Method Application

First, the system consists of only one object with mass (rod). For this object, an arbitrary point needs to specified for the calculations of the potential - and kinetic energies. This point is located along the length of the rod and will be noted as (u_a, z_a) (Figure 2.3). The respective expressions for both u_a and z_a are presented in the form of Equation 2.6 and 2.7.

$$u_a = L_{wire}\, sin(\theta_1(t)) + L_{(u_a,z_a)}\, sin(\theta_2(t)) \tag{2.6}$$

$$z_a = L_{wire}\, cos(\theta_1(t)) + L_{(u_a,z_a)}\, cos(\theta_2(t)) \tag{2.7}$$

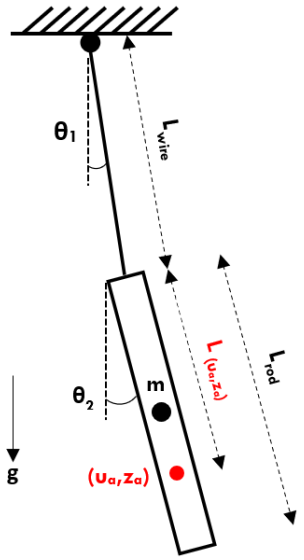

Figure 2.3: Wire-rod System with arbitrary point

The potential - and kinetic energy equations are formulated for the rod by utilising both u_a, z_a, their respective derivatives and integrating all the points along the length L_{rod}. These are expressed in Equations 2.8 and 2.9.

$$P = \frac{m\,g}{L_{rod}} \int_0^{L_{rod}} (L_{wire} - z_a - L_{(u_a,z_a)})\, dL_{(u_a,z_a)} \tag{2.8}$$

$$K = \frac{m}{2\,L_{rod}} \int_0^{L_{rod}} (\dot{u_a}^2 + \dot{z_a}^2)\, dL_{(u_a,z_a)} \tag{2.9}$$

These are then used to calculate the Lagrange equation. The equations of motion for the system is obtained by deriving the equations to the relevant degree of freedom.

In this case, $\ddot{\theta_1}$ and $\ddot{\theta_2}$. The two EoM for this system is presented in Equations 2.10 and 2.11.

$$\ddot{\theta_1}(t) = \frac{g\,(3\,\theta_2(t) - 4\,\theta_1(t))}{L_{wire}} \tag{2.10}$$

$$\ddot{\theta_2}(t) = -\frac{6\,g\,(\theta_2(t) - \theta_1(t))}{L_{rod}} \tag{2.11}$$

2.2.2 Moment Balance Method Application

First, the active forces are identified. These forces are shown in Figure 2.4. Second, the translational acceleration $\ddot{x}$ is calculated using Equation 2.12

$$\ddot{x} = \frac{F_{wire-horizontal}}{m} \tag{2.12}$$

$$\ddot{\theta} = \frac{\mathbf{M}}{\mathbf{I}} \tag{2.13}$$

and 2.13

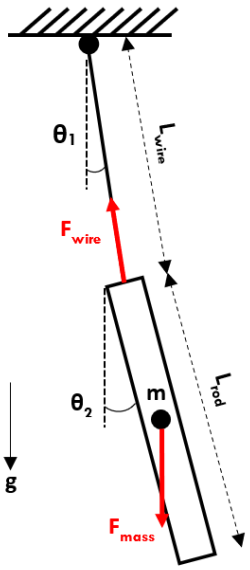

Figure 2.4: Wire-rod System with active forces

Essentially, both methods result in the same equations if elaborated correctly for a particular system. However, considering the fact that the model for this research will be built in MS Excel, the Moment Balance method shows more flexibility when it comes to expanding the model along the way without having to derive a new EoM every time. New external loads can be introduced to the system by simply adding them to the cells responsible for that particular calculation (either the force -or the moment balance). Therefore, the chosen method to describe the motion of the system is the Moment Balance method.

Conclusion: Both method will be tested in the model development phase and the results will be compared.

2.3 Chaos Theory

Chaos theory is a mathematical way of studying systems that are irregular and unpredictable. Its wide applications covers topics like weather forecasting, the financial market, electrical circuits and many more. This theory states that small changes in the current time frame can unpack in a very unexpected way in a future time frame [24]. Therefore, it is not only limited to solely mechanical systems. Kissler even uses this theory to say something about the unpredictability of the Covid-19 pandemic [25]. For dynamical systems this theory implies that what may seem irregular is often just a set of deterministic laws with extreme sensitivity to small changes in the initial conditions. A very well known example of a chaotic dynamical system is the double pendulum. For small motions, the double pendulum is a simple linear system. However, for large motions it generates a very irregular pattern as shown in Figure 2.5.

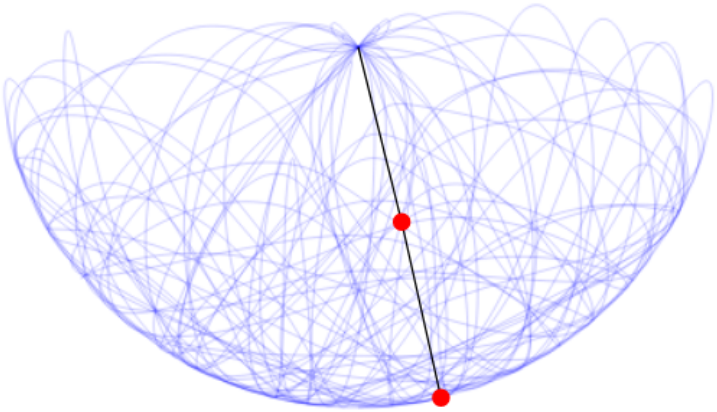

Figure 2.5: Double Pendulum exposed to large motions

An experiment carried out by Livien et al. in 1993 [26] comparing small and large angle motions in a double pendulum experiment clearly shows when large angle motions are involved, the results can easily deviate if only a small change in initial condition is applied.

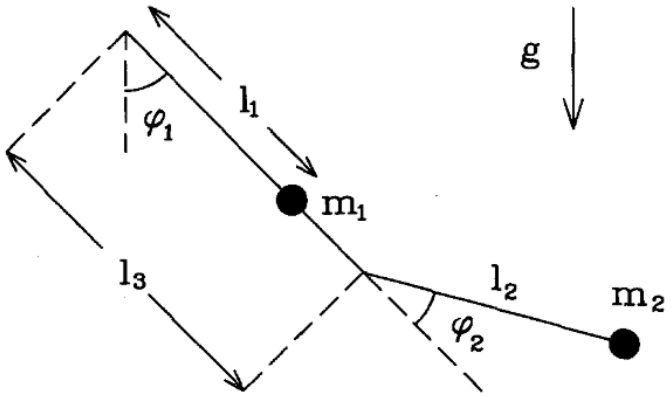

Figure 2.6: Double Pendulum Experiment by Levien et al. [26]

In Figure 2.7 the small angle motions for a double pendulum results in a linear harmonic behavior during the whole simulation. Both angles ϕ_1 (solid line) and ϕ_2 (dashed line) showed stable results without irregularities. Figure 2.7(a) and (b) are the results for the two natural frequencies f_1 and f_2 of the system assuming small angle approximation. These frequencies are obtained by solving the Lagrange equation. Figure 2.7(c) shows the sum of both modes.

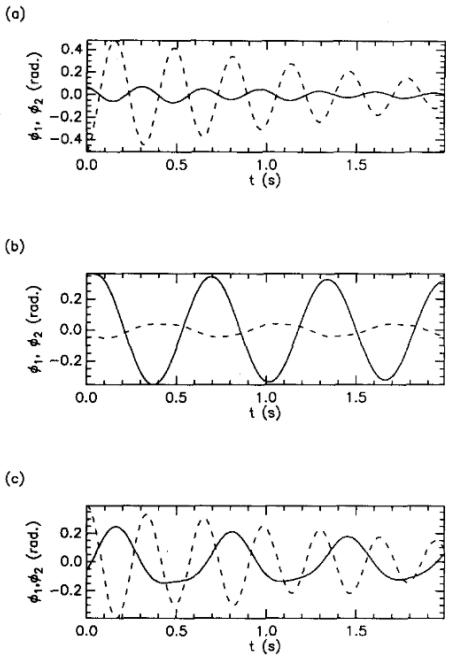

Figure 2.7: Small angle motions [26]

For large angle motions, the results were much more irregular. Figure 2.8(a) represents the angle $\phi 1$ and (b) represent the angle $\phi 2$. The solid line is simulation 1 and the dashed line simulation 2. Both simulations match relatively well in the first 1.5 seconds. However, increasing deviations are seen starting from approximately 1.7 seconds regardless of the fact that both simulations started with very similar initial conditions.

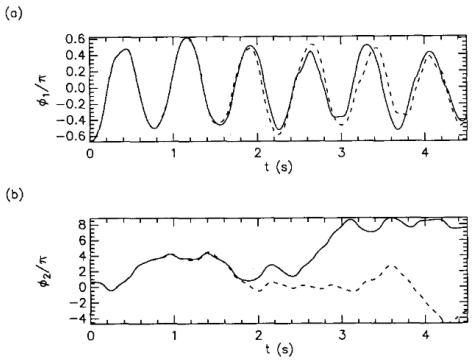

Figure 2.8: Large angle motions [26]

Even though the lifted turbine system is not entirely the same as a double pendulum, it can be concluded from [26] that the motions will behave in a chaotic manner if the initial conditions are not chosen carefully. Therefore, the relevance of this theory to for this thesis is the consideration of a highly potential chaotic situation when the lifted turbine from the crane vessel is exposed to irregular wind - and wave loads causing large angle motions.

2.4 Environmental Conditions

Offshore installations are unique due to its dependence of weather conditions. Procedures are required to be carried out within the determined weather window. Therefore, studying the potentially hazardous environmental conditions offshore wind turbines or other components have to deal with during installation is crucial to a successful and safe process. The two most important environmental limitations affecting the installation process are the local wind speed and sea state [27][28]. Both these parameters are discussed in the next paragraphs.

2.4.1 Wind Wave Correlation

The wind loads which can be encountered offshore plays a crucial and significant role on the offshore structures either during the installation process or the already commissioned wind turbines. For commissioned wind turbines, efficient wind speeds and steadier wind is favorable. However, taking the installation process into account, the opposite situation (lower wind speed or no wind) is more preferable due to the significant impact the wind poses on the crane operations. Especially, when the installation is carried out using a floating vessel with an extremely high crane lifting the turbine tower. The wind load contribution will mostly affect the lowering phase of the lifted tower because this is the phase where the tower has the most freedom in its motions. During the mating phase, this aerodynamic load which is still active over the height of the hoisted tower will result in (potentially large) swinging motions, impact loads, bending moments and vibrations.

An extensive research regarding tower installation carried out by van den Berg, specifically studying the lowering phase until the moment the catcher comes in contact with the MP, shows the significance the present wind spectrum has on the motion of the tower. In certain situation with extreme wind loads, the unpredictability caused by a stochastic spectrum can lead to an unsuccessful mating phase because one of the many installations limits such as impact force or the lifting wire side-lead angle has been surpassed [29]. For this reason, the effect of the wind loads will be taken into account during the calculations and simulations in this research.

The wind speed is not a constant parameter. It varies in both space (wind profile over the height) and time (wind realization). The general reference notation to address the wind speed is U_{10}. This is the mean wind speed (usually measured during 10 minutes) at a height of 10 m above still water level (SWL).

The wave loads on the other hand is not an independent parameter as it is closely correlated with the wind conditions. The waves observed on the free surface is directly a result from the wind blowing over it. For an idealised situation the waves can be modelled with dependency on the wind speed, the fetch (distance between the installation location and the coastline), duration and gravitational acceleration [30]. Al though the idealised wind wave relation might seem way too idealised, it does provide a certain idea of how the wave is affected. A very popular way to predict the dynamics of ocean waves is the WAM model. On a global and regional scale, this model is currently being used to predict sea states. However, this method is by no means perfect and errors will be present to a certain extend. Fortunately, researchers found out that for fully developed sea states, the significant wave height and mean wind speed has the following relation [31]:

$$H_s \sim U_{10}^2 \tag{2.14}$$

With this relation, an estimation can be made for the wave height based on the mean wind speed.

2.4.2 Wind Profile

Given the mean wind speed at 10 m above SWL, the overall wind profile can be estimated by vertical extrapolation. The two most common methods to achieve this profile are logarithmic law (theoretically derived) and the power law (empirically derived) [32].

The *logarithmic law* is expressed as the following (Equation 2.15) [33]:

$$U(z) = \frac{u^*}{k_a} ln \frac{z}{z_0} \tag{2.15}$$

- $U(z)$ - wind speed at height z
- u^* - friction velocity
- k_a - von Karman's constant (k_a = 0.4)
- z_0 - roughness length depending on the type of terrain (open sea with waves, z_0 = 0.0001-0.01)

The *power law* is expressed as the following (Equation 2.16) [33]:

$$U(z) = U(H) \left(\frac{z}{H}\right)^{\alpha} \tag{2.16}$$

- $U(H)$ - mean wind speed at reference height H = 10 m.
- α - Hellmann exponent (open sea with waves, α = 0.12)

For this thesis, there is no specific offshore site chosen to create the model. Therefore, the power law will be used to estimate the wind profile due to its simplicity without having to make an extra assumption for the roughness length z_0 parameter. The Hellmann's exponent α in the power law is equal to 0.12 based on empirical data for an open sea with waves surrounding [33].

Wind Realization

The wind speed over a time-domain can be represented by the following realization as shown below in Figure 2.9.

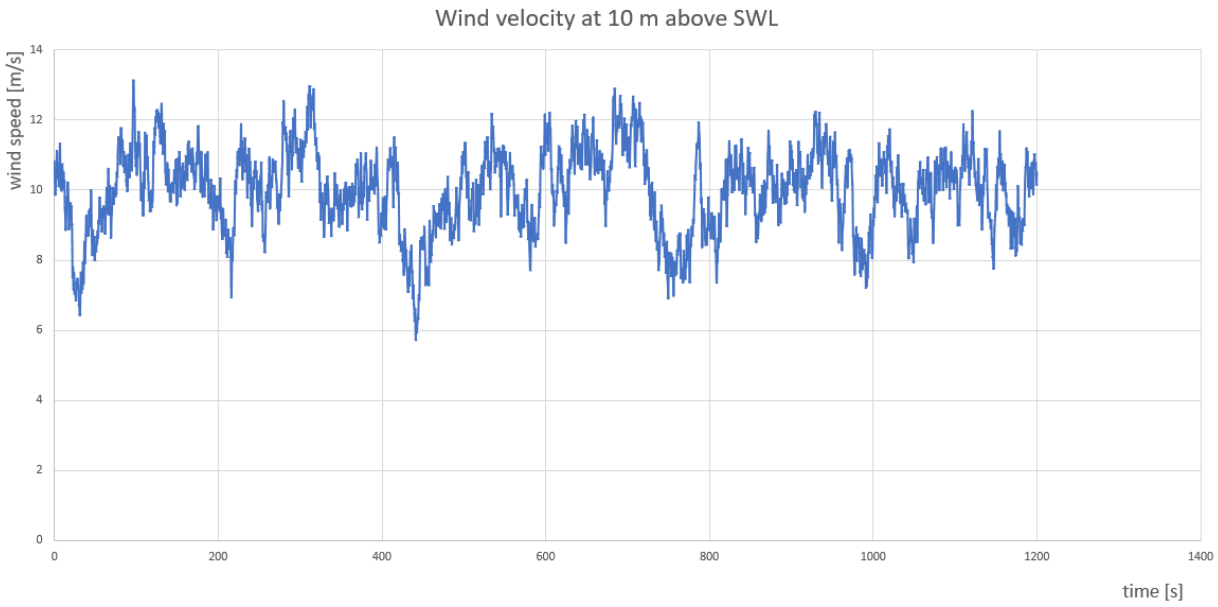

Figure 2.9: Wind speed realization based on hindcast data [29]

This wind velocity graph is determined using hindcast data taking the turbulence aspect into account [29]. This graph is generated from a wind model developed by KCI The Engineers. This model is capable

of delivering 3D wind velocity variations in time for a given offshore surface roughness. This data will be used to model the wind load in the lifted turbine system.

2.5 Vessel to Crane Tip Motions

In this thesis, the motions of the installation vessel itself will be represented by the crane (specifically the tip of the crane) capable of lifting the turbine tower via a lifting wire. Thus, it in important to study the possible motions of the installation vessel itself. These will be translated to the crane tip under the assumption that the connection between the vessel and the crane boom is rigid and one body. The exact model of the vessel is not taken into account in a detailed manner. The motion of this crane tip will be estimated based on the type of vessel, either a jack up or a floating vessel. The six degrees of freedom of a ship is roll, pitch, yaw, surge, sway and heave. This is illustrated in Figure 2.10.

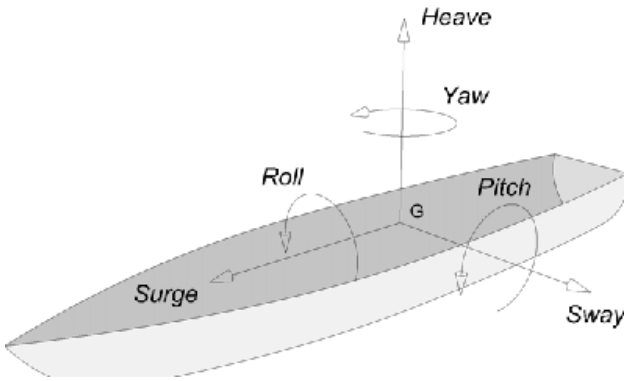

Figure 2.10: Six Degrees of Freedom of a Vessel [34]

For Jack-up vessels all six degrees of freedom are extremely limited making it possible to carry out lifting operations offshore. The legs are fixed on the seabed making this a very stable platform. This is illustrated in Figure 2.11.

Figure 2.11: Jack-up Crane Vessel [35]

Floating DP vessels are less restricted and its motions are more susceptible to external loads. The crane operations will be greatly affected when the environmental conditions are not ideal. Figure 2.12 illustrates a floating DP vessel. Therefore, it can be expected that the motions resulting from a floating vessel in all six degrees of freedom is far greater than those resulting from a bottom fixed jack-up vessel.

Figure 2.12: Floating DP Crane Vessel [36]

In a research carried out by Li et. al in 2013 studying the offshore installation of a MP shows that short waves lead to a more significant response for a jack-up vessel whereas the response of a floating vessel is more sensitive to longer waves due to increasing crane tip motions [20].

2.6 Collision

As described in the thesis formulation, this thesis will cover the investigation of the DSJ mating phase happening under offshore conditions. And the motions of the tower lifted on the top by a wire is very prone to small changes in initial conditions. Therefore, during the mating phase itself, the DSJ rings of the tower will collide a certain number of times with the rings of the substructure. A simple definition of a collision is the occurrence in which two or more object come in contact and apply forces on each other within a relatively short period of time.

2.6.1 Elastic Collision vs Inelastic collision

Two requirements a collision needs to meet to be qualified as elastic is the conservation of both the momentum and the kinetic energy. Therefore, in an elastic collision, all kinetic energy of the moving objects before the collision will still be in the form of kinetic energy after the collision. There will be no energy dissipation in other forms such as sound, heat or vibration (no deformations of the colliding objects will be observed).

An example of a nearly elastic collision is Newton's Cradle. This device is a good demonstration of the principle of the conservation of momentum and energy. It usually consists of a series of metal balls of equal size hanging separately on the same metal frame but just touching each other (at rest) as depicted in Figure 2.13. It is not perfectly elastic because energy is still converted into sound and therefore kinetic energy decreases slowly as time goes by. Apart from the energy being slowly converted into sound waves, this device demonstrates the principle of momentum and kinetic energy conservation quite well and can therefore be categorized as an elastic collision.

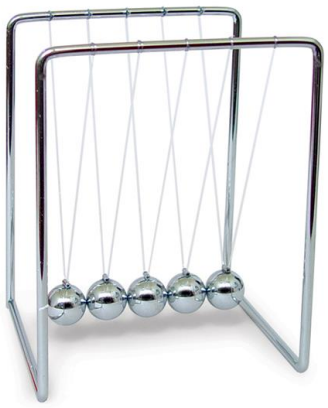

Figure 2.13: Newton's Cradle (also called Newton's Pendulum)

In a perfectly elastic situation, the process of collision will not stop and keeps going on to infinity. However, practically speaking there will always be damping in different forms such as aerodynamic, energy loss in sound waves, heat transfer etc. Eventually, resulting in the system coming at rest. This is where the inelastic collisions comes into the picture.

The conservation of both momentum and kinetic energy is however far from realistic and thus will never be the case with macroscopic bodies. Inelastic collisions are somewhat more realistic in the sense that it accounts for the change in kinetic energy after a collision. In this case, kinetic energy will always be partially converted into other forms mentioned before. The kinetic energy before a collision is greater than that after the collision. It is a matter of time before all kinetic energy of a system is being converted and the system stops moving. Therefore, in an inelastic collision, the conservation of kinetic energy is not valid.

The bouncing ball problem is a well-known example of such a system. Considering the situation where a ball is dropped from a certain height vertically towards the ground, reaches the ground and bounces back upwards. This repeats for several bounces and ultimately the ball comes at rest because of energy being dissipated during collisions. Each time the ball bounces back upwards, it reaches a height less than the previously achieved bouncing height as graphed out in Figure 2.14. The velocity decreases after each bounce until it comes to rest.

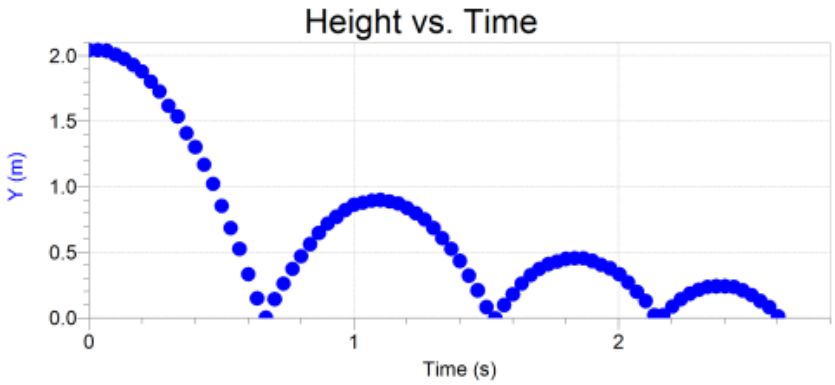

Figure 2.14: Height of bouncing ball in time

2.6.2 Coefficient of Restitution

With the help of a coefficient of restitution (COR), the collisions/impacts that are categorized between perfectly elastic and perfectly inelastic are described. This coefficient ranges from 0 to 1. In literature it is often denoted as **e** or C_R. It is a ratio that covers the change in velocity after a collision between two objects and can be expressed in the following way (Equation 2.17):

$$e = \frac{|v_b - v_a|}{|u_a - u_b|} \tag{2.17}$$

where the numerator represents the relative velocity after a collision between object A and object B and the denominator represents the relative velocity before the collision. This coefficient also accounts for the energy loss after each collision. From the perspective of an inelastic collision it can also be expressed in the form of the kinetic energy before and after a collision (Equation 2.18).

$$e = \sqrt{\frac{\frac{1}{2}mv^2}{\frac{1}{2}mu^2}} \tag{2.18}$$

Of course, this change/loss in energy after a collision depends fundamentally not only on the object's speed but also the material. A research paper on the effects of material properties concludes that the COR is higher for steel than for bronze or aluminium. The experiment was done by dropping bearing balls on three different plates of steel, bronze and aluminium. Two sizes of bearing balls were used to test the effect of geometry as well. The results shows that the COR is not a constant value and changes depending on the velocity. In Figure 2.15 the results are plotted for all three prisms (each with two ball radii tests) against a dimensionless velocity. This velocity is a ratio between the current velocity and the velocity at maximum impact. This paper proves that the COR is a linear relation for large impact velocities. And the smaller ball bearing results in greater COR values compared to the bearing with larger radii [37].

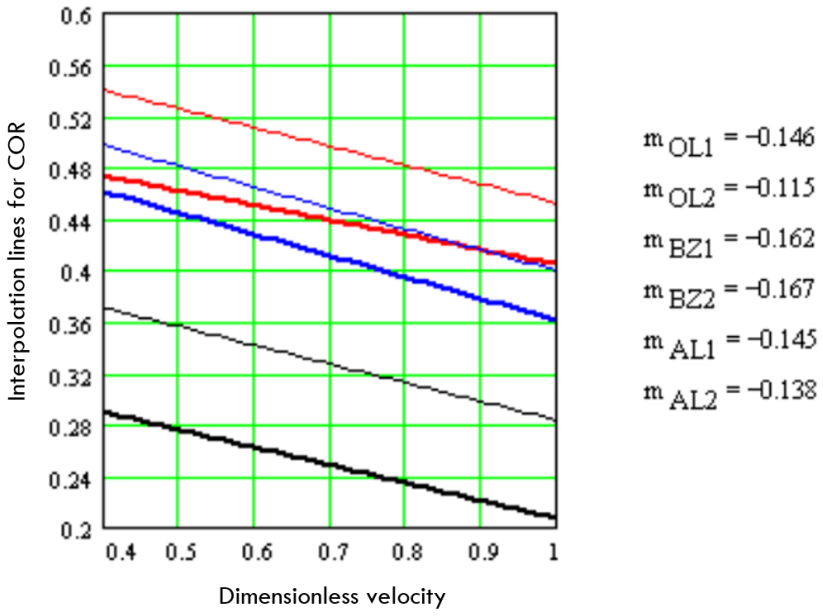

Figure 2.15: Interpolated COR and slope values for steel, bronze and aluminium and the two different bearing balls [37]

2.7 Collision detection

Although a collision might seem straightforward in mathematical calculation, additional effort is required when it comes to modelling the collision scenario in any software or more practical applications. In literature, collision detection is widely applied in fields such as robotics, computer simulations, game development and dynamic simulations. The fundamental principle of a collision detection system is to limit the object's motion by applying dynamic boundary conditions. An accurate detection system is required in order to anticipate realistic collision response. In a simulation, this part is considered to be the most challenging. The collision phase is built up of three major parts: the detection, defining the contact area and obtaining the collision response.

There are many ways to model a detection system to check whether two or more objects are intersecting or not. In the field of robotics, collision is detected using a path-planning algorithm. Two alternatives will be reviewed in the following paragraphs:

- The GJK algorithm with Minkowski difference
- Line-Line Intersection

The GJK Algorithm
The foundation of the GJK algorithm is based on the Minkowski difference. This Minkowski difference of two convex shapes A and B can be determined by taking a set of differences of the position vectors. It can be noted in the following way (Equation 2.19 [38]):

$$A \ominus B = \{a - b : a \in A, b \in B\} \tag{2.19}$$

An example is illustrated in Figure 2.16 where two objects are considered in the xy-plane along with their calculated Minkowski Difference illustrated by the dashed line.

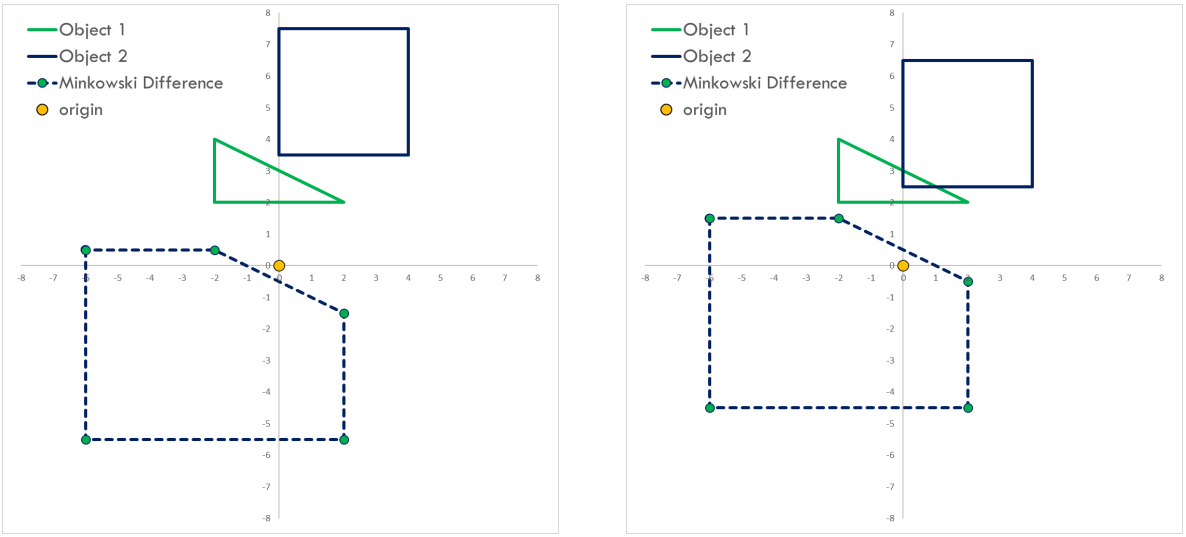

(a) No collision **(b)** Collision

Figure 2.16: Minkowski Difference of two objects

In the left figure (Figure 2.16a) no collision is detected between the two objects. The origin is outside the boundaries of the Minkowski difference. In the right figure2.16b) there is overlap between the object, which indicates a collision. Note that the origin now is within the boundaries of the Minkowski

difference. This is a property of the Minkowski difference: for an intersection to be valid, this difference always contains the origin [39].

However, it is not the most efficient way to calculate the difference for all the position vectors when the object are moving constantly in time (especially when complex convex shapes are involved). This is where the GJK algorithm comes in. This algorithm only checks whether the difference contains the origin or not by defining specific points of the object and using direction vectors. This is an iterative process to determine the shortest distance between a point from the Minkowski difference and the origin. Figure 2.17 gives an idea how the GJK iterative algorithm works for finding that shortest distance to the origin O.

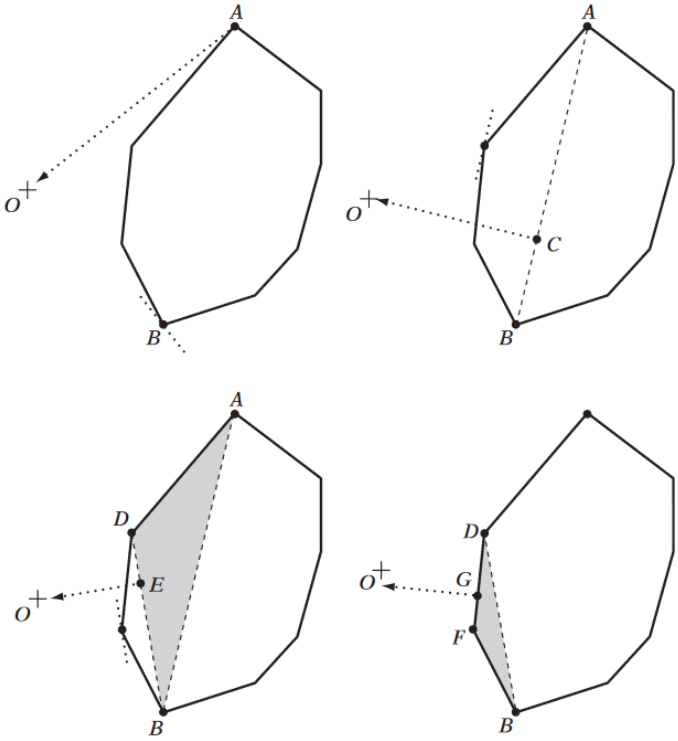

Figure 2.17: GJK iteration to find the closest point on the object to the origin [38]

However, according to [39] the GJK algorithm is not considerable due the fact that it only works with convex shapes. Therefore, another approach will be reviewed following this method.

Line-Line Intersection

This approach is purely based on the mathematical way determining whether two lines are intersecting or not. When given two random lines in a 2D space, the three possibilities are:

- 0-point in common: parallel lines
- 1-point in common: intersecting lines
- all points in common: coinciding lines (both share the exact same properties)

Given the equation of the two lines (Equation 2.20 and 2.21, the intersection point can be determined using Equation 2.22.

$$y = a_1 x + b_1 \tag{2.20}$$

$$y = a_2 x + b_2 \tag{2.21}$$

$$P_{intersect} = (\frac{b_2 - b_1}{a_1 - a_2}, a_1 \frac{b_2 - b_1}{a_1 - a_2} + b_1) \tag{2.22}$$

After reviewing the above methods from literature, a decision has been made for the method to be implemented to solve the collision detection problem. As mentioned above, the GJK algorithm works optimally with convex shapes. The model of this research involves a rather complex 2D shape of the DSJ on the tower and the MP with concave characteristics. Solving this with the splitting method might lead to an increase in computational time for each simulation. The line-line intersection method can not be directly applied as well because these are considered lines with infinite lengths. Applying this to a scenario consisting of objects of finite length will need a modified version of the method. A possible solution to convert the infinite length issue to a finite one is to make use of the Excel software's programming functions to set the boundaries for each line. Therefore, a modified version of the more simplistic approach of line-line intersection will be used for collision detection in the model.

2.8 Mating Requirements

Before the mating phase of the DSJ itself, the tower is lowered until the first impact happens. The limiting parameter for this lowering phase of the WTG tower is studied extensively in a research done by M. van de Berg [29]. Parameters such a slack wires, optimized catcher types, maximum impact forces, wind velocities etc. are investigated. The goal is to align the tower and the MP and make sure the conditions are all within their allowable limits to carry on with the mating phase of the DSJ [29]. The crucial field of study regarding the mating phase of the DSJ is the assessment of potential structural damage by means of FEM models. This damage can be assessed by studying the impact forces between the DSJ connection from the tower and the MP. The aim is to find a critical value for the maximum impact force which leads to unwanted damage or structural failure. This maximum impact force can then be translated to more practical parameters such as impact velocity and bending moments [40].

Structural damage can also be assessed by checking if certain impact forces lead to equivalent stresses above the yield limit of the material. Failure theories can be applied to assess or predict damage. For brittle (e.g. concrete) materials, the definition of failure is when fracture occurs. For ductile (e.g. steel) material, plastic deformation is the critical parameter.

The widely used failure theory for ductile (metals) materials is the von Mises stress criterion. This criterion states that if the calculated von Mises stress is greater than the yield limit stress of the material, the structure will yield and plastically deform. The von Mises stress calculation is used in many professional finite element analysis softwares e.g. SimScale, ABAQUS and Ansys. Therefore, the von Mises yield criterion will be applied in this thesis to assess the impact forces and stresses from the model simulations.

Bibliography

[1] WindEurope, "Wind energy in Europe in 2018 - Trends and statistics," *Trends and statistics*, p. 32, 2019.

[2] E. Sesto and N. H. Lipman, "Wind energy in Europe," 2020.

[3] M. D. Esteban, J. S. López-Gutiérrez, V. Negro, and L. Sanz, "Riprap scour protection for monopiles in offshore wind farms," *Journal of Marine Science and Engineering*, vol. 7, no. 12, pp. 1–18, 2019.

[4] TNO, "Design Limitations For Future Very Large Monopiles."

[5] X. Wu, Y. Hu, Y. Li, J. Yang, L. Duan, T. Wang, T. Adcock, Z. Jiang, Z. Gao, Z. Lin, A. Borthwick, and S. Liao, "Foundations of offshore wind turbines: A review," *Renewable and Sustainable Energy Reviews*, vol. 104, pp. 379–393, apr 2019.

[6] IRENA, "Floating Foundations: A Game Changer for Offshore Wind Power," pp. 1–8, 2016.

[7] J. Taboada, "Comparative analysis review on Floating Offshore wind Foundations (FOWF)," *Ingeniería naval*, no. 949, pp. 75–87, 2016.

[8] M. Leimeister, A. Kolios, and M. Collu, "Critical review of floating support structures for offshore wind farm deployment," *Journal of Physics: Conference Series*, vol. 1104, p. 012007, oct 2018.

[9] C. Li, Z. Gao, T. Moan, and N. Lu, "Numerical simulation of transition piece - Monopile impact during offshore wind turbine installation," *Proceedings of the International Offshore and Polar Engineering Conference*, vol. 3, pp. 370–375, 2014.

[10] B. E. Burton Tony, Jenkins Nick, Sharpe David, *Wind Energy Handbook*. John Wiley & Sons, 2 ed., 2011.

[11] P. Schaumann, S. Lochte-Holtgreven, and F. Wilke, "Bending tests on grouted joints for monopile support structures," in *Proceedings of the 10th German Wind Energy Conference (DEWEK), Bremen, Germany*, 2010.

[12] N. I. Tziavos, H. Hemida, N. Metje, and C. Baniotopoulos, "Grouted connections on offshore wind turbines: a review," *Proceedings of the Institution of Civil Engineers - Engineering and Computational Mechanics*, vol. 169, no. 4, pp. 183–195, 2016.

[13] A. Mehmanparast, S. Lotfian, and S. P. Vipin, "A review of challenges and opportunities associated with bolted flange connections in the offshore wind industry," *Metals*, vol. 10, no. 6, 2020.

[14] P. Dallyn, A. El-Hamalawi, A. Palmeri, and R. Knight, "Experimental testing of grouted connections for offshore substructures: A critical review," *Structures*, vol. 3, pp. 90 – 108, 2015.

[15] M. L. Segeren, E. M. Lourens, A. Tsouvalas, and T. J. Van Der Zee, "Investigation of a slip joint connection between the monopile and the tower of an offshore wind turbine," *IET Renewable Power Generation*, vol. 8, no. 4, pp. 422–432, 2014.

[16] M. L. Segeren and K. W. Hermans, "Experimental investigation of the dynamic installation of a slip joint connection between the monopile and tower of an offshore wind turbine," in *Journal of Physics: Conference Series*, vol. 524, Institute of Physics Publishing, 2014.

[17] A. Semiari, "An alternative for the conventional grouted connection of monopile support structure for offshore," 2015.

[18] N. Visser, "Experimental set-up of the Double Slip Joint," 2015.

[19] Y. Xiao, "No TitleDesign Optimization of Rolled Double Slip Joint Based on Scale Experiments and FEM," 2017.

[20] L. Lin, Z. Gao, and T. Moan, "Numerical Simulations for Installation of Offshore Wind Turbine Monopiles Using Floating Vessels," pp. 1–11, 2013.

[21] A. S. Verma, Z. Jiang, N. P. Vedvik, Z. Gao, and Z. Ren, "Impact assessment of a wind turbine blade root during an offshore mating process," *Engineering Structures*, vol. 180, pp. 205 – 222, 2019.

[22] A. S. Verma, Z. Jiang, Z. Ren, Z. Gao, and N. P. Vedvik, "Response-based assessment of operational limits for mating blades on monopile-type offshore wind turbines," *Energies*, vol. 12, no. 10, pp. 1–26, 2019.

[23] Excelunusual, "http://www.excelunusual.com/,"

[24] MathVault, "The Definitive Glossary of Higher Mathematical Jargon - Chaos."

[25] K. Stephen and B. Resnick, "How chaos theory helps explain the weirdness of the Covid-19 pandemic," 2020.

[26] R. B. Levien and S. M. Tan, "Double pendulum: An experiment in chaos," *American Journal of Physics*, vol. 61, no. 11, pp. 1038–1044, 1993.

[27] Lillgrund, "Experiences from the Construction and Installation of Lillgrund Wind Farm," *Distribution*, no. May, 2008.

[28] E. Uraz, "Offshore Wind Turbine Transportation & Installation Analyses. Planning Optimal Marine Operations for Offshore Wind Projects," *Master Thesis*, p. 56, 2011.

[29] M. van den Berg, "Limits of Offshore Wind Turbine Installation with the Double Slip Joint," 2020.

[30] L. H. Holthuijsen, *Waves in Oceanic and Coastal Waters*. Cambridge University Press, 2007.

[31] P. Janssen, "The wave model May 1995 By," *Training*, no. May 1995, 2003.

[32] S. Emeis and M. Turk, "Comparison of Logarithmic Wind Profiles and Power Law Wind Profiles and their Applicability for Offshore Wind Profiles," *Wind Energy*, no. December, pp. 61–64, 2007.

[33] G. Kovacs, "Environmental conditions and environmental testing," *INTELEC, International Telecommunications Energy Conference (Proceedings)*, vol. 2, no. October, pp. 92–99, 1993.

[34] J. M. Varela and C. Soares, "Interactive simulation of ship motions in random seas based on real wave spectra," in *GRAPP*, 2011.

[35] Maritimetechnology, "Soul jack-up vessel - The next step for offshore wind," 2017.

[36] Energyfacts.eu, "Offshoretonic Releases a New Offshore Installation Vessel Design," 2020.

[37] F. C. CIORNEI and S. ALACI, "the Effects of Geometry and Material Properties on the Coefficient of Restitution," *ANNALS OF THE ORADEA UNIVERSITY. Fascicle of Management and Technological Engineering.*, vol. XXIII (XIII), 2014/1, no. 1, pp. 10–14, 2014.

[38] C. Ericson and M. Kaufman, *Real-Time Collision Detection*. 2005.

[39] S. Kockara, T. Halic, K. Iqbal, S. Member, C. Bayrak, and R. Rowe, "Collision Detection : A Survey," vol. 72205, pp. 4046–4051, 2007.

[40] W. Guachamin Acero, L. Li, Z. Gao, and T. Moan, "Methodology for assessment of the operational limits and operability of marine operations," *Ocean Engineering*, vol. 125, no. August, pp. 308–327, 2016.

(This is a modified version of the report and only consists of the first two chapters due to confidential reasons.)